



**US Army Corps
of Engineers**

Engineer Research and
Development Center

Technical Report ITL-99-5
December 1999

Computer-Aided Structural Engineering (CASE) Project

Rivet Replacement Analysis

by Erich Edward Reichle

Approved For Public Release; Distribution Is Unlimited

20000309 044

Prepared for Headquarters, U.S. Army Corps of Engineers

DTIC QUALITY INSPECTED 3

The contents of this report are not to be used for advertising, publication, or promotional purposes. Citation of trade names does not constitute an official endorsement or approval of the use of such commercial products.

The findings of this report are not to be construed as an official Department of the Army position, unless so designated by other authorized documents.



PRINTED ON RECYCLED PAPER

U.S. Army Engineer Research and Development Center Cataloging-in-Publication Data

Reichle, Erich Edward.

Rivet replacement analysis / by Erich Edward Reichle ; prepared for U.S. Army Corps of Engineers ; monitored by U.S. Army Engineer Research and Development Center, Information Technology Laboratory.

89 p. : ill. ; 28 cm. — (Technical report ; ITL-99-5)

Includes bibliographical references.

1. Rivets and riveting — Computer programs. 2. Riveted joints — Computer programs. 3. Corrosion fatigue — Computer programs. 4. Finite element method — Computer programs. I. United States. Army. Corps of Engineers. II. U.S. Army Engineer Research and Development Center. III. Information Technology Laboratory (U.S.) IV. Computer-aided Structural Engineering Project. V. Title. VI. Series: Technical report ITL ; 99-5.
TA7 E8 no.ITL-99-5

PREFACE

This report presents an analysis of the behavior of deteriorated rivets used in connections of structural steel members. Specifically, the effect of material loss due to corrosion is assessed by finite element analysis. The results of a parametric study and recommendations for replacement criteria for deteriorated rivets are provided.

This report is a thesis in partial fulfillment of the requirements for the degree of Master of Science in Civil Engineering, University of Central Florida, Orlando, FL.

This report was written by Erich E. Reichle. Funding for this project was provided by the Computer-Aided Engineering Division (CAED), Information Technology Laboratory (ITL), U.S. Army Engineer Research and Development Center (ERDC), under the Computer-Aided Structural Engineering (CASE) Project. Mr. H. Wayne Jones was Chief, CAED, and Mr. Timothy D. Ables was Acting Director, ITL.

At the time of publication of this report, Dr. Lewis E. Link was Acting Director of ERDC, and COL Robin R. Cababa, EN, was Commander.

The contents of this report are not to be used for advertising, publication, or promotional purposes. Citation of trade names does not constitute an official endorsement or approval of the use of such commercial products.

TABLE OF CONTENTS

LIST OF TABLES	vi
LIST OF FIGURES	vii
CHAPTER I - INTRODUCTION	1
Organization and Content	1
Problem Statement	2
Research Issues, Objective and Benefits	4
Modeling Methods	5
CHAPTER II - LITERATURE REVIEW	6
Rivet History	6
Installation of Rivets	7
Structural Connection Behavior	9
The Corrosion Process	12
Mechanical Properties	15
Finite Element Method	17
Symmetric and Non-Symmetric Corrosion	18
CHAPTER III - FINITE ELEMENT MODEL	19
Model Development	19
Computer Program	20
Elements Used	22
Validity of Mesh	23

Boundary Conditions	24
CHAPTER IV - STUDY OF STRESS LEVELS IN A DETERIORATING RIVET	26
Applied Loads	26
Observations - Uniform Model	26
Observations - Non-Uniform Model	27
Material Loss Thresholds	27
Variation of Load Distribution Along the Rivet Head	31
CHAPTER V - CONCLUSIONS AND RECOMMENDATIONS	34
Replacement Criteria for Tension Rivets	34
Correlation to Other Loading Conditions	35
Recommended Procedure for Evaluating a Riveted Connection	37
Future Work	38
APPENDICES	39
A. Uniform Model Stress Contours	40
B. Non-Uniform Model Stress Contours	62
REFERENCES	76

LIST OF TABLES

Table 1 - A502 Rivet Steel Hardness Requirements	16
Table 2 - $\frac{7}{8}$ -inch Button Head Rivet Dimensions	19
Table 3 - Steel Properties Used	21
Table 4 - Computed Stresses (Uniform Model)	29
Table 5 - Computed Stresses (Non-Uniform Model)	30

LIST OF FIGURES

Figure 1 - Corroded rivets at St. Lucie Lock	3
Figure 2 - Corroded rivets at Palm Valley Bridge	3
Figure 3 - ANSI Rivet Head Types	8
Figure 4 - Connections in Pure Shear	10
Figure 5 - Connections in Pure Tension	10
Figure 6 - Connections in Combined Shear and Tension	11
Figure 7 - Stress-Strain Diagram Used for Rivet Steel	21
Figure 8 - Axisymmetric Element Stresses	22
Figure 9 - Typical Finite Elements	23
Figure 10 - FEM Boundary Conditions (Uniform Model)	25
Figure 11 - FEM Boundary Conditions (Non-Uniform Model)	25
Figure 12 - Max. Stress Vs. Loss of Head Volume (Uniform Model)	29
Figure 13 - Max. Stress Vs. Loss of Head Volume (Non-Uniform Model)	30
Figure 14 - Rivet Head Load Distribution FEM Boundary Conditions	31
Figure 15 - Normal Stress Distribution vs. Distance From Rivet Shank	33
Figure 16 - Tension/Allowable Deterioration Interaction	36

CHAPTER I

INTRODUCTION

Organization and Content

This thesis consists of five chapters. The first defines specific problems relating to rivet deterioration and the issues that pertain to it. Also discussed are the objectives of this work, and its anticipated benefits and applications. Concluding this chapter is a brief discussion of the modeling methods used to approximate the physical condition of an installed and deteriorating rivet.

Chapter II contains a review of prior studies performed on rivet deterioration and topics relating to the validity of this research. These topics include the history of rivets in the United States, the behavior of different structural connections, the mechanical properties of steel rivets, and the development of a finite element model to analyze the performance of deteriorating rivets under static loading.

Chapter III presents in detail how a $\frac{7}{8}$ -inch diameter button head rivet is modeled numerically. The finite element program used to create the model is discussed to include the selection of the mathematical elements, mesh topography (number of elements), and boundary conditions used.

With the computer model defined, Chapter IV investigates the behavior of a deteriorating rivet. Service loads are applied, and a parametric study is undertaken to determine relationships between material loss and stress levels within the rivet.

Lastly, Chapter V draws conclusions from the research. Benefits gained from the work are also noted and possible areas of future work are addressed.

Problem Statement

Structures generally consist of individual members that are connected together to serve a useful purpose. For any structure to perform successfully, the connections as much as the main load carrying members must be in adequate condition to handle the stresses experienced by the system. Periodic maintenance and rehabilitation of steel structures are necessary throughout their useful life. For if they are not, the loss of a sizeable capital investment and human life can result. The lifespan of a structure varies as a function of how well it is maintained and its exposure to unusual and extreme occurrences. Since riveted connections were widely used in older structures currently in need of repair, there is particular interest in the effect of material loss due to corrosion in rivets. Connection performance can be significantly affected depending on its type, configuration, degree of wear, and amount of rivet material loss.

The inspection of riveted connections joining steel structures has revealed rivet head deterioration varying from zero to one-hundred percent. Figure 1 is a photograph showing a series of corroded rivets in a steel frame which forms the lower sector gate of St. Lucie Lock in Stuart, Florida. Figure 2 is a photograph showing corroded rivets used to connect plates which form the bascule girders of the Palm Valley Bridge in St. Johns County, Florida. Conditions such as these present concerns in evaluating the integrity of structures and raise questions such as: Will the deteriorated rivet heads be able to hold the connection tight? Is there a minimum acceptable amount of rivet head

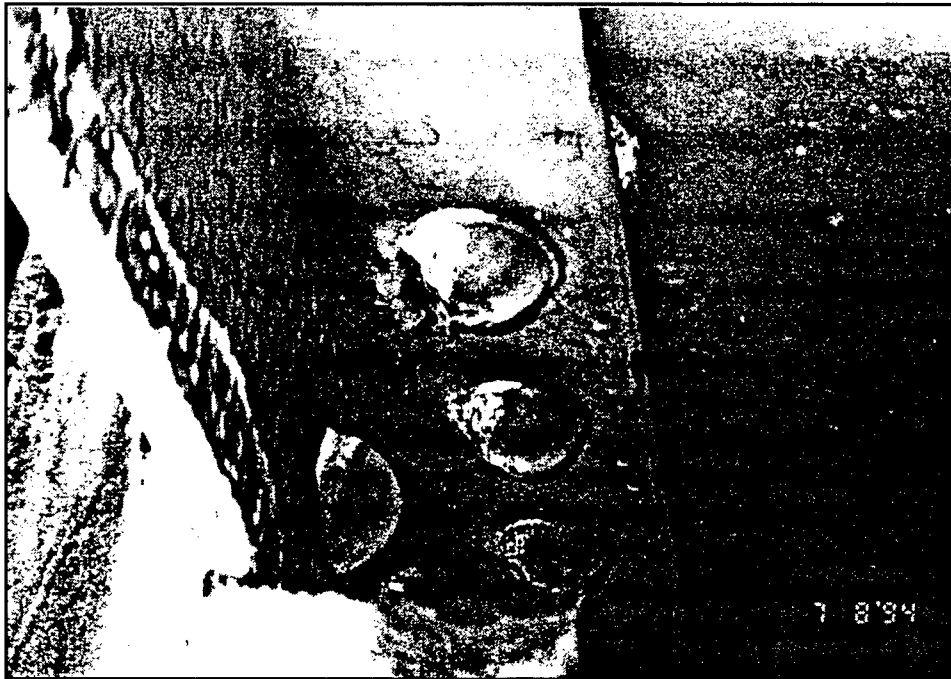


Figure 1 - Corroded rivets at St. Lucie Lock

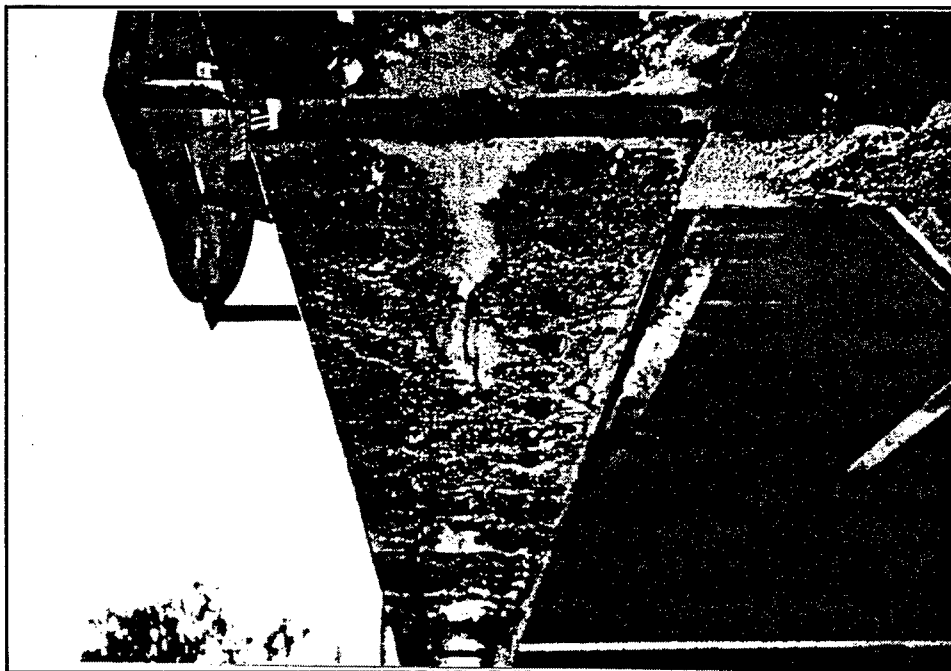


Figure 2 - Corroded rivets at Palm Valley Bridge

loss? Does the type of loading influence this minimum acceptable amount? Can uniform replacement guidelines be established to aid inspectors and design engineers in preparing maintenance work plans and specifications?

In the case of St. Lucie Lock, the importance of correctly evaluating these situations is even more crucial. Unlike structures such as the Palm Valley Bridge which can be visually inspected on a regular basis, opportunities to inspect locks such as this in a "dewatered" condition are infrequent. The normal immersion of the structure in its corrosive, salt water environment can cause problems that seem small during inspection to develop into larger ones later when they cannot be seen.

Research Issues, Objective and Benefits

The research issues in this thesis specifically pertain to the effects of progressive rivet head corrosion on the stress distribution in a $\frac{7}{8}$ -inch diameter steel button head rivet. Different support condition assumptions at the rivet head-base plate interface are included. Also, the influence of connection type (i.e., shear, tension, combined) is addressed.

The primary objective of this research is to determine, quantitatively, an amount of rivet head material which may be lost without compromising the integrity of the connection of which it is a part. Current practice has been to replace all rivets in connections subjected to tensile or tensile-shear loading that have heads corroded to the point of losing 50% or more of their lip (projection beyond the shank) [7]. This criteria is arbitrary though, and from this research it is anticipated that specific guidelines for rivet replacement can be established which will reduce the subjectivity in assessing

borderline cases for repairs.

Modeling Methods

A two-dimensional axisymmetric finite element model of a $\frac{7}{8}$ -inch diameter button head rivet will be developed to investigate the effects of uniform, progressive corrosion on the internal stress distribution. Since the amount of material projecting beyond the shank develops stresses when the rivet is in tension, there should be a correlation between deterioration and stress within the rivet. These relationships will be used to determine a point at which small losses of rivet head material cause significantly large and unsafe increases in stress within the rivet.

CHAPTER II

LITERATURE REVIEW

A literature review on the topic of deteriorating rivets and replacement criteria found that very little information exists. In fact, only one paper could be located that specifically addressed it. Fazio and Fazio [7] presented a paper at the Second Bridge Engineering Conference, Washington, DC, which discussed problems the New Jersey Transit Corporation is having in evaluating their 600 railroad bridges. Their goal was to develop rivet replacement criteria which are simple, reliable, reproducible, and can be used as a guideline by the engineer during inspection and subsequent rehabilitation. They addressed the mechanical aspects of the problem including loading conditions and failure modes, as will this paper. The inspection and replacement criteria they developed were only qualitative in nature though, and they concluded that *"further studies should attempt to determine the amount of rivet head reduction that would be acceptable to maintain service loads."*

Rivet History

The use of rivets and riveting techniques to assemble materials together has been dated as far back as biblical times [3]. Their use today can still be observed, although not as frequently as 20 to 30 years ago. Rivets were the most commonly used fastener in the early days of steel construction, but even then bolts made of mild carbon steel

were also used. The ability of rivets to expand and fill holes during installation made them the perfect type of fastener for bridges and buildings since these structures required tight fitting connections. In the 1920's welding techniques began to improve, but rivets were still preferred over welded construction because their requirements and limitations were better understood. In 1951, the American Society for Testing and Materials (ASTM) issued its first specification for structural joints using high-strength bolts. Since then, the use of structural rivets has steadily declined and today they are rarely used except in historical restoration projects such as the Aberjona River Bridge in Winchester, Massachusetts [16]. The extinction of rivets can be largely attributed to the intense labor involved in their installation. A quality job, much like masonry work, depended a great deal on the skills of the construction laborers. The work had to be closely inspected and any rivets which were found to be improperly installed had to be cut out and replaced. Conversely, high-strength bolts can be installed in a relatively short amount of time with unskilled labor and much less quality control.

Installation of Rivets

Rivets used in construction were a soft grade steel which remained ductile after being heated. The usual rivet consisted of a solid, cylindrical shank with a manufactured head on one end. The current American National Standard for rivets $\frac{1}{2}$ -inch nominal diameter or larger (ANSI B18.1.2 - 1972) [17] recognizes six types of manufactured heads, the most common being the button head (see Figure 3). The rivet was heated in the field to a cherry-red color (approximately 1800 - 2300°F), inserted into the hole and a head formed on the blunt end with a pneumatic rivet gun. The gun was fitted with the

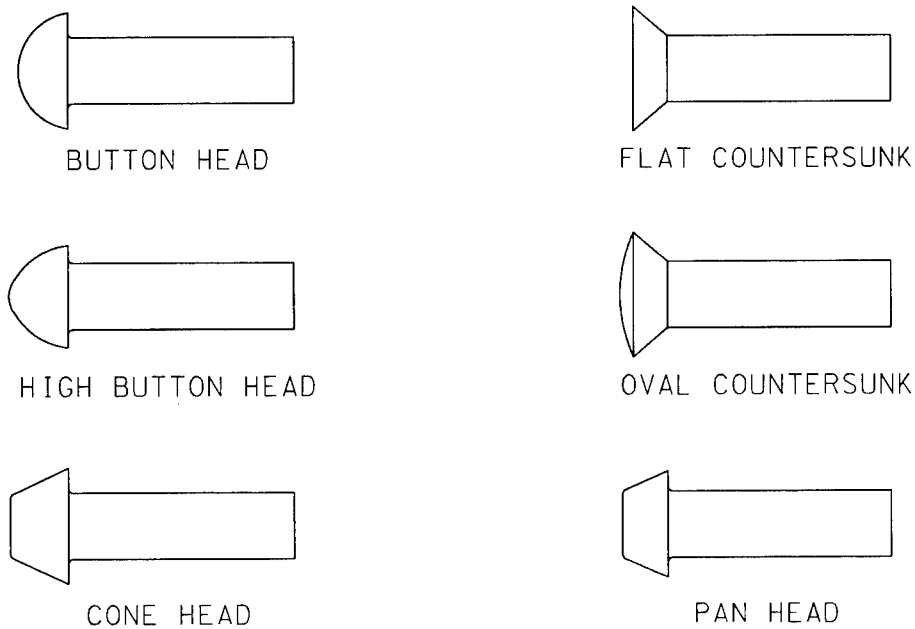


Figure 3 - ANSI Rivet Head Types

proper die to form the head by rapid, successive blows to the rivet. Shop riveting was done in the same fashion except the rivet was driven in one stroke with a pressure type riveter. This riveter compresses the rivet with a force between 50 to 80 tons, causing the rivet to expand and fill its hole almost completely making a tighter connection. This is why shop riveting is preferred. As the rivet cools it shrinks and creates a clamping force between the parts it connects. Measurements have shown this force to approach the yield load of the rivet [13,15]. This residual force contributes to the frictional resistance of the connection, but unlike high-strength bolts which are torqued to a specific pre-tension, this force is unpredictable and is not included in the design strength of a connection.

Structural Connection Behavior

Among the various connections which are used to join structural steel members, there are three significant loading conditions to which they can be subjected. These are pure shear, pure tension, and combined shear and tension.

When the lines of action between connected members are parallel, their fasteners are in "pure shear" (see Figure 4). Though there may be some eccentricity introduced by the geometry at the connection, it is not significant. In this type of joint the rivets tend to be sheared off along the planes of contact between the members. If the members are arranged so that the rivet shear force is divided up evenly between more than one plane of contact, the load-carrying capability of the rivet is theoretically increased by the number of shear planes. In this situation the function of the rivet head is nominal. The only concern is that it can keep the connection snug and prevent the rivet from possibly working loose.

Figure 5 shows a typical connection where rivets are in pure tension. Until about 1930, many engineers had strongly objected to using rivets in tension loadings for fear that the rivet heads might be pulled off. This fear was unjustified though and results of tests published that year by Oliver and Wilson [15] at the University of Illinois showed that they were reliable in tension loadings. Axial tension in fasteners occurs in a tension member whose line of action is perpendicular to the connecting member. When a tension load is applied, the initial precompression of the connected members is reduced. If this load does not exceed the precompressive load, the force in the rivet will equal the applied tensile force plus any remaining contact forces. Increases in external load

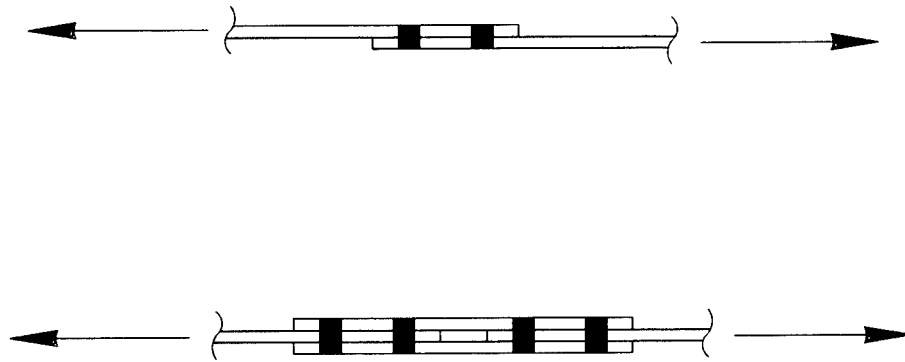


Figure 4 - Connections in Pure Shear

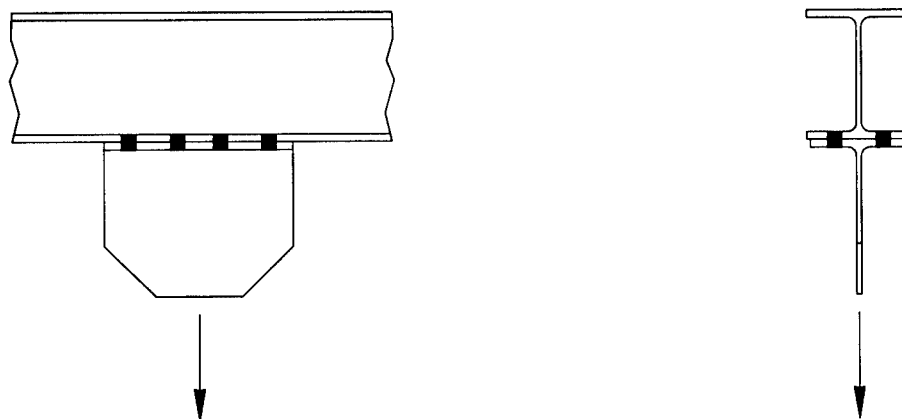


Figure 5 - Connections in Pure Tension

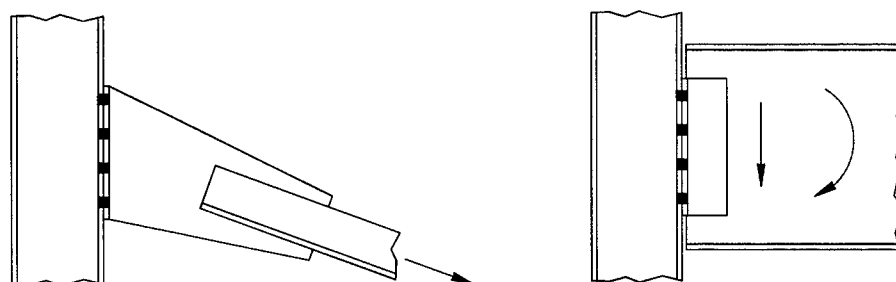


Figure 6 - Connections in Combined Shear and Tension

beyond that point will totally relax the contact forces, and the tension in the rivet will equal the applied load. This assumes the rivet heads are full and provide the area needed to develop the restraining force. It also assumes there is no restraint derived from friction between the shank and the connecting material which seems logical. When hot driven rivets which are initially compressed during installation begin to cool, they contract both longitudinally (providing a clamping force) and radially due to the Poisson effect. This radial contraction presumably eliminates most of the contact, and therefore the friction between the shank and the connecting material. Photographs showing sawed sections of hot driven rivets of different sizes and grip lengths clearly demonstrate this point [8]. When the tension member is not perpendicular to the connecting member (a

more common situation), the fasteners are subjected to both axial tension and shear.

In most commonly used connections, the effects of both shear and tension must be considered to adequately design them. Figure 6 shows some typical connections that are affected by both shear and tension. In these types of connections the vertical component of load being transferred is resisted by the shear strength of the rivets. The horizontal component is resisted by the rivet tensile strength. An elliptical interaction curve can adequately describe the strength of rivets under combined tension and shear [8]. It is used to relate the shear stress component to the critical tensile stress component. Again, as in the case of the pure tensile load, the rivet head is relied upon to restrain the connecting material and enable the rivet to fully develop the required stress.

The Corrosion Process

Since the condition of the rivet head has been shown to be an important factor in the performance of connections subjected to pure tension and combined shear and tension, it is prudent to review how their deterioration takes place. Depending on the function of the structure, the type of steel used in its construction, and the level of corrosion protection used, the rivet head could possibly be degraded in several ways [4].

In general, these can be categorized as:

1. General atmospheric corrosion
2. Localized corrosion
3. Mechanically assisted corrosion

General atmospheric corrosion is characterized by slow, symmetrical, uniform

thinning of the material. It usually occurs in normal ambient conditions. This type of corrosion is not considered crucial, although it can progressively build and present problems over long periods of time. Any unexpected failures from this form of corrosion can usually be avoided by regular inspection. It is the most commonly encountered type of corrosion and is the easiest form to measure [10].

Localized corrosion occurs at certain areas within a structure and proceeds at a faster rate than general corrosion. There are at least five types of localized corrosion which can possibly occur. They are crevice corrosion, pitting corrosion, galvanic corrosion, stray-current corrosion, and filiform corrosion.

As the name implies, crevice corrosion is found in small openings along the perimeter of contact surfaces between members. It typically occurs at crevices between connected plates, or more relevant to this study, at a rivet head-connecting plate interface. The environmental conditions in a crevice tend to be more aggressive than those of a clean, open surface. Small volumes of solution containing deposits will stagnate in the openings (usually a few thousandths of an inch or less) and initiate a corrosive attack [9].

Pitting corrosion is defined by small indentations or "pits" which penetrate into the material. This type of corrosion can cause severe, localized loss of member cross-sectional area including holes. The pits can have various shapes and sizes which may contribute to their continual growth in much the same manner as crevice corrosion [10].

Galvanic corrosion can occur when steels of different electrochemical potentials are joined. The larger the potential difference, the more chance of galvanic corrosion.

Since oxidation is accelerated in the material with the higher potential (the anode), it is necessary to make rivets and other fasteners with small surface areas less electrochemically active than their connecting plates. This is done by alloying them with other metals such as nickel, copper, and chromium [2].

Stray-current corrosion can occur if electrical currents are conducted along improper paths in structures. Notable examples are welding generators and cathodic protection systems [18]. If electrical currents from these systems are grounded through moist soil or water, corrosion at areas where these currents enter and leave the structure can occur.

Filiform corrosion (also known as underfilm corrosion) initiates at points of failure in paint systems designed to inhibit corrosive attack. It is observed as random lines of corrosion underneath the paint film which originate from the source of the defect. It is an unusual type of attack since it does not weaken or destroy metal components, but merely affect surface appearance. It is a result of paint system failure [4,9,18].

Mechanically assisted corrosion also occurs, although less frequently than general and localized corrosion. It is usually associated with hydraulic structures and consists of three types. They are erosion corrosion, cavitation corrosion and fretting corrosion [4,9,10,18].

Erosion corrosion is caused by the removal of material due to the impacts of particles. These particles are carried by fluids and usually have a specific direction of movement associated with them. Most of the time this movement is very rapid. This

type of corrosion can be recognized by initial paint removal (in painted structures) followed by identifiable imprints due to the particles causing the erosion.

Cavitation corrosion is a special form of erosion corrosion caused by the formation of negative pressures such as those developed during high-velocity turbulent flows. These pressures tend to remove any surface treatments and expose the unprotected metal. This makes the metal highly susceptible to corrosion. Cavitation damage is acknowledged as being a result of both corrosion and mechanical effects.

Fretting corrosion is a combination of frictional wear and subsequent corrosion. It results when small vibrational motions occur between surfaces. It also is a special form of erosion corrosion. Red rust is formed and is observable at the contact surfaces. The amount of relative motion necessary to produce fretting corrosion is very small (displacements as small as 10^{-8} cm) [9]. This type of corrosion is likely to occur if rivets become loose and their connections are subjected to some degree of cyclical loading.

Mechanical Properties

Rivets are made from bar stock and their heads manufactured by either hot or cold forming. Current specifications identify three types of structural rivet steels. ASTM specification A502 [2] grade 1 rivet steel is made from a low carbon steel and is intended for general applications. It is slightly weaker than ordinary A36 steel and has more ductility. Rivets made from this steel were used in almost all structural work where they were used as fasteners, including construction with high-strength steels. ASTM A502 grade 2 rivet steel is made from a carbon-manganese alloy. It has a higher strength than grade 1, is less ductile, and was developed for use with higher strength

yield stress ($0.6 F_y$.)

Finite Element Method

The finite element method (FEM) used in structural analysis is an approximate method usually based on an assumed displacement field [12]. The approach is to divide a continuous medium into a finite number of regions using basic geometric shapes. Key points on these individual elements are selected as nodes where equilibrium conditions and continuity of displacement are maintained. Mathematical functions for each element degree-of-freedom (usually its nodal displacements) are assumed which relate the displacement at any point on the element to nodal displacements. Stress-strain and strain-displacement relationships in each element are employed to develop element stiffness equations, the relationships among nodal internal forces and nodal displacements. Corresponding element stiffness coefficients and equivalent nodal loads are determined using virtual work or strain energy principles. Finally, equilibrium equations for the nodes are written and continuity of the nodal displacements is enforced which allows the formulation of global stiffness equations, the relationship among the applied nodal loads and nodal displacements for the structure as a whole. When structural restraints are imposed, the global stiffness equations may be solved for the nodal displacements. From these displacements the element stresses and structure reactions can be determined.

For modeling purposes a rivet head can be defined as an axisymmetric solid. That is, a three-dimensional body that is developed by the rotation of a planar section about an axis. If the loads applied to the rivet are also axisymmetric, it can be analyzed

by the FEM using only a representative two-dimensional section.

Symmetric and Non-Symmetric Corrosion

As discussed earlier in this chapter, the most prevalent form of corrosion is general atmospheric corrosion. It is also the easiest form to measure. Although it is understood that situations involving non-symmetric material loss do occur, and that they presumably are more serious, an analysis simulating the symmetrical corrosion of rivets will provide results applicable to the majority of cases encountered. Additionally, recommendations for replacement based on a minimum remaining uniform area criteria can be applied in the field with a high degree of reliability. The use of a symmetrical deterioration pattern also enables the rivet to be modeled using only one-half of its geometry.

CHAPTER III

FINITE ELEMENT MODEL

Model Development

Since the most commonly used rivets were either $\frac{3}{4}$ or $\frac{7}{8}$ -inch button head [13], it was decided to develop a model of the latter. The dimensions used for the head and shaft were the basic values obtained from ANSI B18.1.2 as demonstrated in Table 2. The shaft grip length "L", can vary depending on the size of plates being connected. A 1-inch grip length (two - $\frac{1}{2}$ -inch thick plates being joined) was assumed since it is commonly encountered in construction. The specification also requires that all rivets,

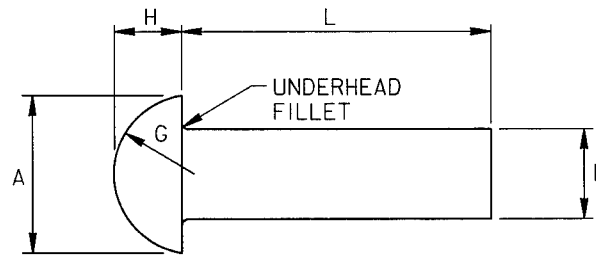


Table 2 - $\frac{7}{8}$ -inch Button Head Rivet Dimensions

Shank Diameter E (in.)	Head Diameter A (in.)	Head Height H (in.)	Head Radius G (in.)
0.875	1.531	0.656	0.775
Source: The American Society of Mechanical Engineers (1972).			

other than countersunk head types, be furnished with a definite underhead fillet with a radius not to exceed 0.062 inch. For this reason, a 0.03125 ($1/32$) inch fillet was used.

Mechanical properties assumed for the rivet model were those of A502 grade 1 steel. However, a yield stress of 30 ksi is used instead of the undriven value of 28 ksi. This value relates better to the allowable stress of 23 ksi in the AISC specifications. Using the Von Mises yield criterion for multi-axial states of stress, any elements in the rivet which have yielded during the investigation are modeled to follow a piecewise linear strain hardening path as shown in Figure 7. Table 3 summarizes all mechanical properties used.

Computer Program

NISA, which stands for Numerically Integrated elements for System Analysis, is a general purpose finite element program developed and supported by Engineering Mechanics Research Corporation [6]. It has the ability to analyze a wide range of engineering mechanics problems. The most notable for this situation are the linear elastic and elasto-plastic material models coupled with linear and non-linear static analyses. Solution techniques employ a matrix wavefront minimization algorithm, and offer a choice between conventional and modified Newton-Raphson iterative methods for solving non-linear problems.

Pre- and post-processing are achieved through the use of **DISPLAY III**, the sister program to **NISA**. Included in its pre-processing (model creation) repertoire is an automeshing feature [5]. This feature enables the user to quickly develop a topography using the geometric boundaries of the element being modeled. Element sizes can be

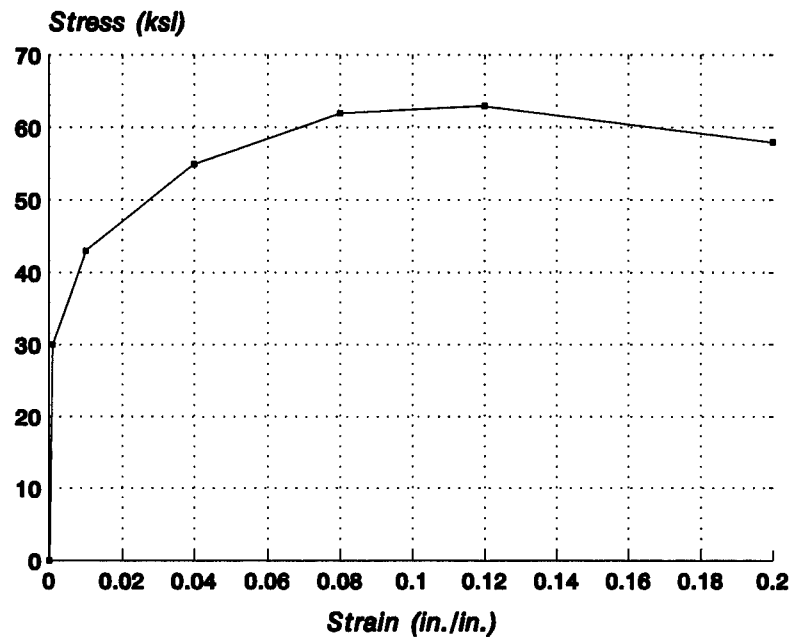


Figure 7 - Stress-Strain Diagram Used for Rivet Steel

Table 3 - Steel Properties Used

Property	Value
E, Young's Modulus	29,000 ksi
ν , Poisson's Ratio	0.3
G, Shear Modulus	11,150 ksi
F_{y2} Yield Stress	30 ksi

made uniform or can be graded to densify smaller areas. Output features are comprehensive and can be tailored to meet individual requirements. Displacements, reactions, internal forces, strain energy, and stresses (principal, maximum shear, Von Mises, octahedral shear) can all be reported. Various geometry plotting features are

available and contour plots for displacements and stresses can be done.

Elements Used

NISA contains a library of many types of finite elements. Each element is defined by two variables - type and order. The element type used to model the rivet is an axisymmetric solid. Its use is based on the assumption that the geometry, material properties, loadings and corrosion loss of the structure being modeled are all rotationally symmetric. It has two degrees-of-freedom per node (displacement in the r and z directions). Figure 8 shows that its state of stress is defined by axial stresses in all three coordinate directions (σ_r , σ_z , σ_θ), shear stress along the r face in the z direction (τ_{rz}) and shear stress along the z face in the r direction (τ_{zr}). The element order specifies its shape and number of nodes. The axisymmetric element used is isoparametric which means the polynomial function used to describe its shape also relates its nodal and

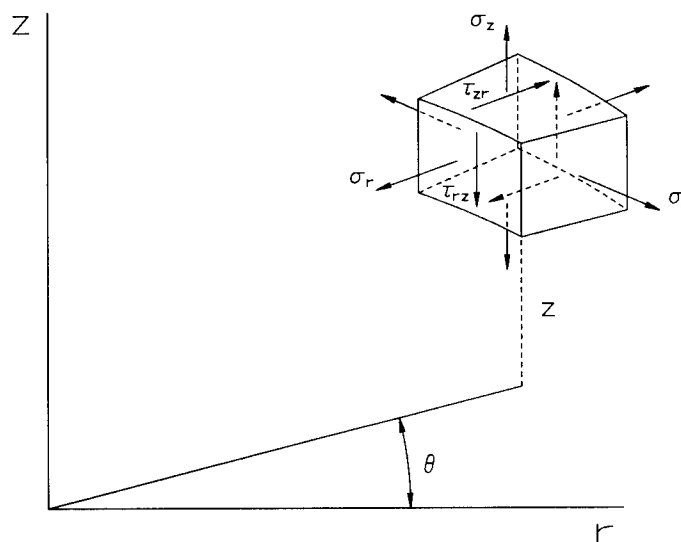


Figure 8 - Axisymmetric Element Stresses

element displacements. Quadrilateral shapes with 4 to 12 nodes or triangles with 3 or 6 nodes can be defined (see Figure 9). The geometry of the quadrilateral is almost as good as the triangle for modeling irregular boundaries, but quadrilaterals generally give more accurate results than triangles [12]. The reason being that a quadrilateral usually has more nodal displacements than a triangle. As such, its assumed displacement functions can be of higher order and thus more accurate. The element order used for the rivet model is an 8 node quadrilateral.

Validity of Mesh

In developing a finite element mesh arrangement, the number of elements used should be increased in regions with high stress gradients. Elements should be of regular shape whenever possible. This is achieved when the element aspect ratio (length:width) is approximately equal to 1. Since the objective of the research is to determine a minimum acceptable percentage of remaining rivet head area, the number of elements used must also be sufficient to degrade the model in small enough intervals to find

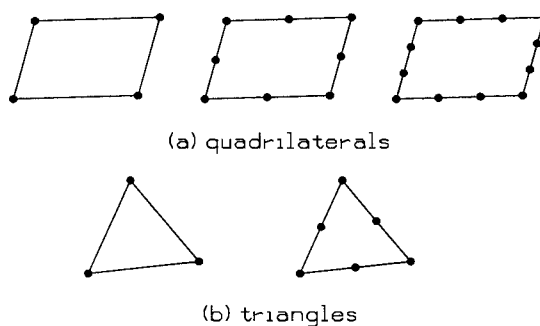


Figure 9 - Typical Finite Elements

this critical area.

The **DISPLAY III** automesh feature described earlier was used to develop two distinct models. The first is designed so that elements can be removed in uniform, concentric layers which imitates the condition of general atmospheric corrosion. For the second model an arbitrary, non-uniform pattern of elements is created. This pattern is used to simulate the localized corrosion condition. In both cases, the removal of a layer of elements causes a reduction in the rivet head volume. Uniform size elements of approximately $1/32$ -inch in size are used along the circumference of the rivet head boundary and around the junction between the shank and head. Using this size enables each model to be degraded in small enough intervals to bound the solution. It is also reasonable to assume that this increment is the smallest value that can be measured accurately in the field. Elements farther away from stress concentration areas are increased in size to reduce model complexity and subsequent computer processing time.

Boundary Conditions

Since the force distribution at the rivet head-connecting plate interface is uncertain when a deteriorated rivet is loaded, it is necessary to evaluate different assumptions for the reaction distribution. Each model is constrained to allow for no translation in the z direction along every node at the end of the shank and no translation in the r direction for all nodes along the axis of symmetry (see Figures 10 and 11). This satisfies the axisymmetric condition and likely the effects of a tight fitting shank in the rivet hole. It also permits different load distributions to be applied along the underside of the head which simulate how the connecting plate and rivet head may interact.

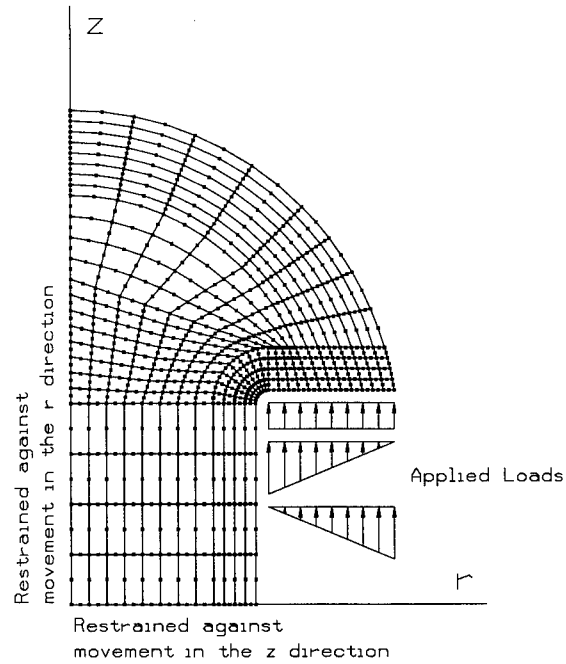


Figure 10 - FEM Boundary Conditions (Uniform Model)

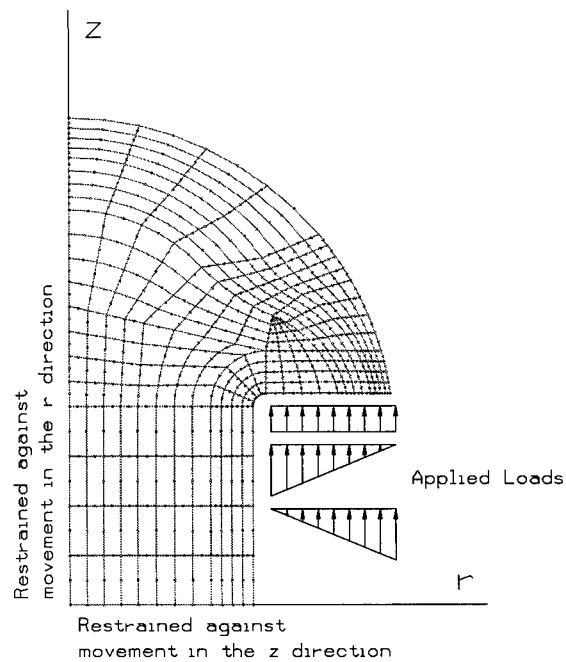


Figure 11 - FEM Boundary Conditions (Non-Uniform Model)

CHAPTER IV

STUDY OF STRESS LEVELS IN A DETERIORATING RIVET

Applied Loads

To determine an acceptable amount of rivet head reduction to maintain service loads, both models developed in Chapter III are loaded along the underside of the lip projection with an equivalent pressure equal to 13.8 kips. This is the allowable load for a $\frac{7}{8}$ -inch grade 1 rivet in pure tension given by AISC. Three forms of pressure are investigated: uniform, triangular-linearly decreasing from the shank and triangular-linearly increasing from the shank. As elements which comprise the bearing surface of the rivet are removed to simulate corrosion, the pressures are adjusted to equate to the applied load. In each case, the equivalent pressure is maintained while layers of the rivet head are removed and stress levels determined.

Observations - Uniform Model

Appendix A contains stress contours plots for the rivet at increasing, nominal levels of deterioration for all three loading conditions used. In general, all three cases begin with a small zone of yielded elements around the area of the underhead fillet, even with a full head (0% deterioration). As the removal of material progresses, this zone of yielded elements grows until the ultimate stress is reached. At this point it is presumed that a crack develops and failure occurs.

It can also be noted in each of the stress contour plots that the rivet head acts as a compression ring (or hemisphere in 3-D) when loaded. In each case a definite volume of low stress elements (the gray area) is formed. It separates the shank which is in tension from the rivet head which is in compression.

Observations - Non-Uniform Model

Appendix B contains stress contours in the rivet at increasing, nominal levels of deterioration for all three loading conditions used. As with the uniform model, all three cases begin with a zone of yielded elements around the area of the underhead fillet. As before, the zone continually grows until the ultimate stress is reached and failure occurs.

There is, however, a notable difference in how the stress is distributed within the rivet head due to the non-uniformity of the material loss. It can be seen how the void of material which had before acted as a compression ring, causes a significant increase in the level of stresses in the rivet head. This is clearly demonstrated by the rapid failure of the linearly increasing pressure case.

Material Loss Thresholds

For correlation purposes, it is necessary to standardize how the material loss in the rivet head is measured. The most consistent method to use would be the total rivet head volume. The percent deterioration for this method is calculated as:

$$\%Deterioration = \frac{V_o - V}{V_o} \times 100$$

where V_o = initial volume
 V = remaining volume

The nominal values used to categorize the stress contour titles in the appendices are based on 10% of deterioration for each layer of elements that is removed.

Table 4 lists the maximum Von Mises stresses achieved for each load case at each level of deterioration investigated using the uniform model. The data are also presented in graphical form in Figure 12. Referring to the graph, a well-defined point can be extracted at which the maximum stresses begin to rise sharply with very small increases of material loss. Up to this point, the maximum stresses have only increased approximately 7% from their value with a full rivet head. For the uniform pressure case, this point occurs at approximately 43% loss of total head volume. For the linearly decreasing pressure case it occurs at 41%, and for the linearly increasing pressure case it is roughly 28%.

Table 5 lists the maximum Von Mises stresses achieved for each load case at each level of deterioration investigated using the non-uniform model. The data are also presented in graphical form in Figure 13. As before, a well-defined point can be extracted for the uniform and linearly decreasing pressure cases. For both cases it occurs at approximately 36% loss of total head volume. However, for the linearly increasing pressure case, the model shows absolutely no tolerance for material loss. A definite point of rapid stress increase cannot be identified.

Table 4 - Computed Stresses (Uniform Model)

% Deterioration		Maximum Von Mises Stress* (ksi)		
Nominal	Total Volume	Uniform	Linearly Decreasing	Linearly Increasing
0	0	37.38	37.62	41.67
10	10	37.62	37.97	42.08
20	19	38.02	38.68	42.93
30	28	38.24	39.56	43.82
40	36	38.49	40.91	49.49
50	43	39.36	44.46	57.08
60	50	47.73	57.82	**
70	57	60.79	**	**
* $F_y = 30$ ksi, $F_u = 60$ ksi ** Solution did not converge				

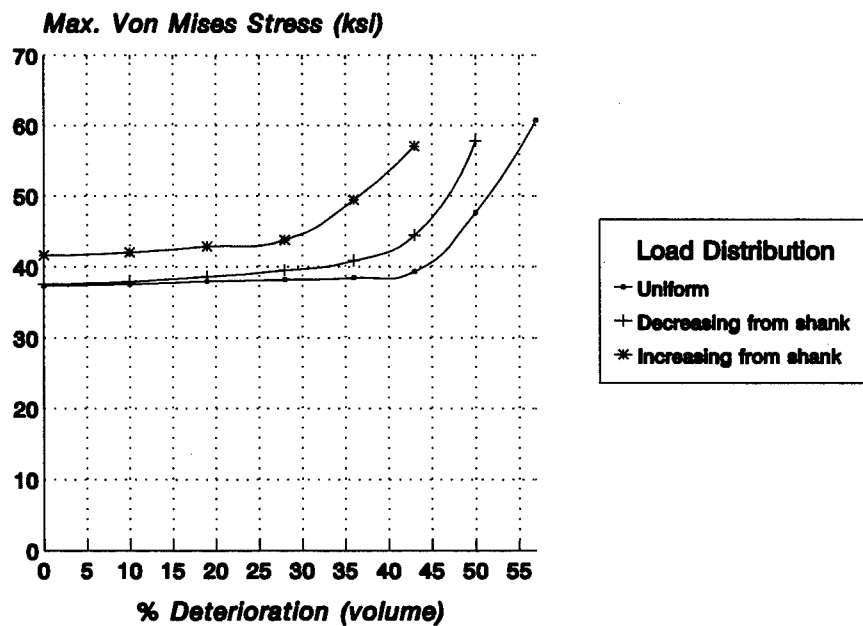
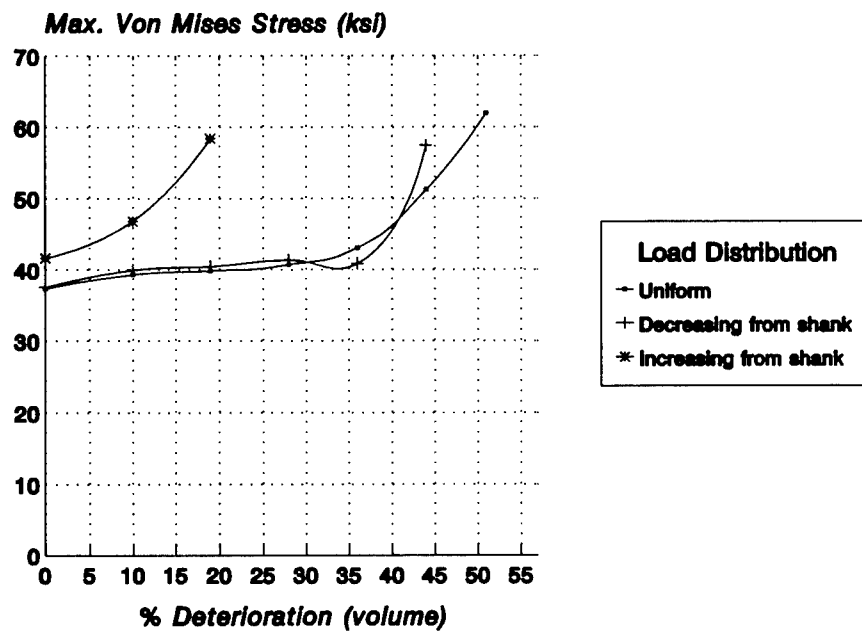


Figure 12 - Max. Stress Vs. Loss of Head Volume (Uniform Model)

Table 5 - Computed Stresses (Non-Uniform Model)

% Deterioration		Maximum Von Mises Stress* (ksi)		
Nominal	Total Volume	Uniform	Linearly Decreasing	Linearly Increasing
0	0	37.38	37.62	41.67
10	10	39.39	40.01	46.84
20	19	39.89	40.50	58.48
30	28	40.76	41.40	**
40	36	43.11	40.91	**
50	44	51.27	57.49	**
60	51	61.96	**	**
70	57	**	**	**
* $F_y = 30$ ksi, $F_u = 60$ ksi ** Solution did not converge				

**Figure 13 - Max. Stress Vs. Loss of Head Volume (Non-Uniform Model)**

Variation of Load Distribution Along the Rivet Head

Although the three loading distributions used in the stress level investigation can bound the possible behavior of a deteriorating tension rivet, it is unclear which type of distribution is most likely to occur. In order to better understand the variation of load distribution along the rivet head, the uniform axisymmetric finite element model was used. For this investigation the boundary conditions were modified by allowing no translation in the z direction at every node along the underside of the rivet head, and no translation in the r direction for all nodes along the axis of symmetry as before (see Figure 14). This permits a uniform pressure of 23 ksi (the equivalent to a 13.8 kip allowable tension load) to be applied along the rivet shank, and the normal stress

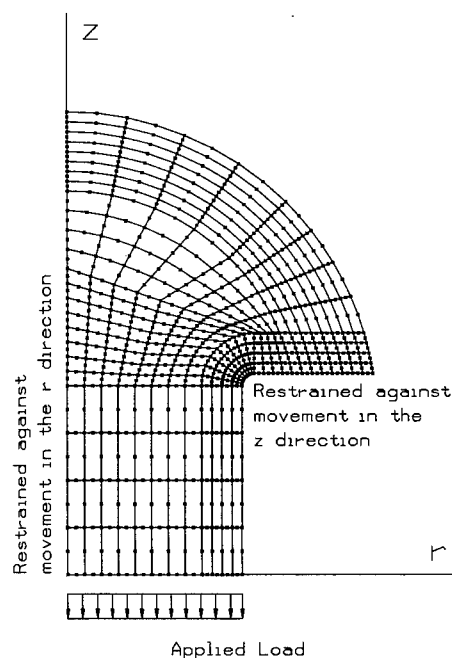


Figure 14 - Rivet Head Load Distribution FEM Boundary Conditions

distribution (σ_z) along the underside of the head to be determined at each nominal level of corrosion.

Results of the study are presented in Figure 15 as graphs of the normal stress distribution versus the distance from the rivet shank. Each plot shows a strong correlation to the triangular-linearly decreasing distribution. Beginning with no material loss (a), the distribution appears to be exponentially decreasing from the shank. As the deterioration progresses, it approaches the linearly decreasing case. This holds true up until the point at which failure is about to occur (g). Here, the distribution displays a modest range of uniformity.

From these results it can be reasoned that the triangular-linearly increasing case is a severe and unlikely situation. Therefore, its influence on determining replacement criteria should be limited if not eliminated. In this study, however, it must be emphasized that any effect the connecting plate stiffness has on the distribution is neglected.

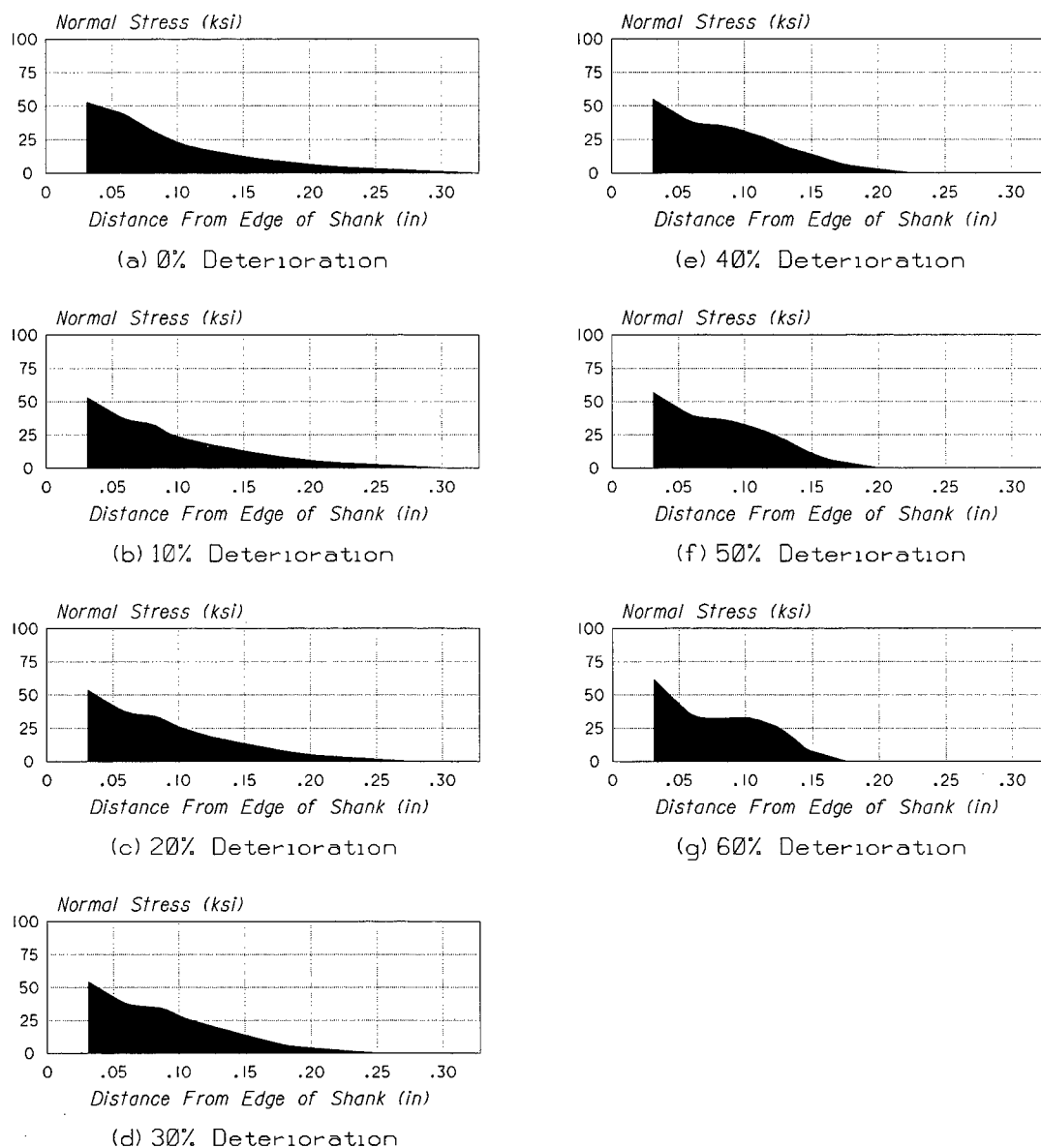


Figure 15 - Normal Stress Distribution Vs. Distance From Rivet Shank

CHAPTER V

CONCLUSIONS AND RECOMMENDATIONS

Replacement Criteria for Tension Rivets

When the amount of rivet head material which can be lost before service load stresses become too large has been identified, replacement criteria can be more confidently defined. If one assumes that the load distribution between the rivet head and the connecting plate behaves predominately triangular-linearly decreasing as was shown in Chapter IV, it is logical to use the average between the critical values determined for both the uniform and non-uniform models under this loading, coupled with a factor of safety (FS) as the basis for recommending when a tension rivet should be replaced. Using the total head volume measurement, and a $FS = 1.1$, one obtains an allowable value of 35%.

Application of this value must take into consideration the corrosion history (rate) of the connection, its frequency of inspection, and the number of rivets that it has. For example, one might consider a tension connection such as the one shown in Figure 5 (see page 10). Hypothetically, all 8 of the rivets over a period of 5 years have corroded to the point of losing 30% of their total head volume. The structure is only inspected once a year. Even though the rivets are currently under the recommended value of 35%, the average corrosion rate is 6% per year. This means there is a good possibility that all the rivets will not meet the criteria by the time they are inspected the

next year. Although the connection contains 8 rivets (i.e., there is some redundancy), all of them are significantly corroded. If the situation were that only 4 of the 8 rivets were corroded 30%, the tendency might be to wait an additional year before considering replacement of the 4 rivets.

Correlation to Other Loading Conditions

As described in Chapter II under the Structural Connection Behavior section, the three significant loading conditions a rivet experiences are pure shear, pure tension, and combined shear and tension. For the pure tension case, the physical condition of the rivet head has been shown to be vital in the performance of such connections, and a maximum corrosion volume has been suggested. In the case of pure shear, the condition of the rivet head is not as crucial. In such situations, the replacement criteria recommended by Fazio and Fazio [7] appear sufficient. They suggested that as long as there is some partial head beyond the rivet hole, the corrosion has not extended into the shank, and the rivet is not loose, it can be considered satisfactory and need not be replaced.

For the more common situation of rivets subjected to combined shear and tension, a rational approach would be to assume an interaction equation between the percentage of head deterioration and the percentage of force (tension + shear) applied to the rivets as tension. Using a straight line relationship (see Figure 16), one observes that as the percentage of force that is applied as tension increases, the tolerable percentage of head loss decreases. This relationship creates a region where all possible combinations of rivet tension load and head volume deterioration are acceptable. This area is bounded

by the arbitrary maximum amount of material loss that can be tolerated and still keep the rivet tight in pure shear (here taken to be 95%) and the recommended allowable

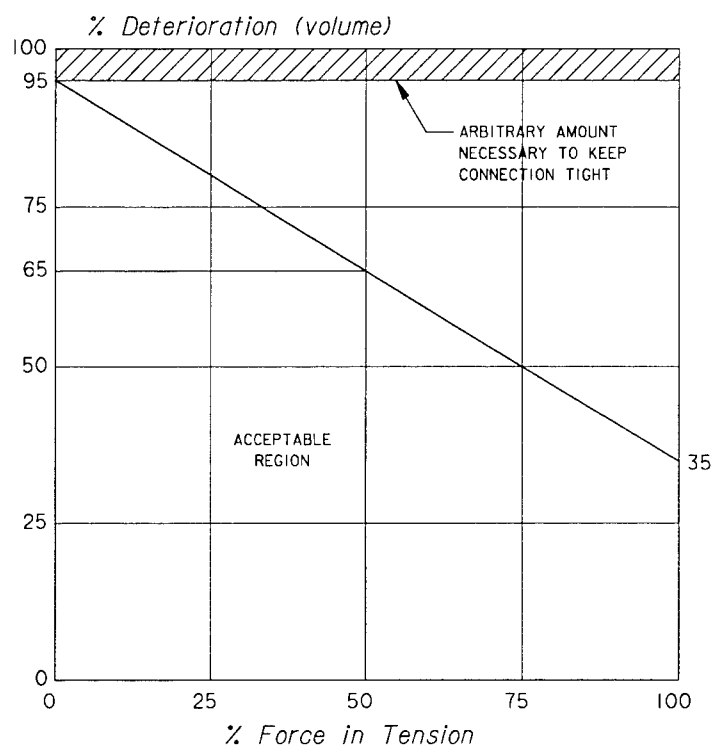


Figure 16 - Tension/Allowable Deterioration Interaction

percentage of total head volume deterioration for pure tension (35%).

One can consider, for example, some wind bracing connected as shown in the left side of Figure 6 (see page 11). Assume the geometry of the bracing is such that the force in each rivet is same in both shear and tension (i.e., the bracing is at a 45° angle). Using Figure 16, one observes at the intersect of the 50% point on the x-axis, there is an allowable deterioration of approximately 65%. Application of this value is also

dependent upon the evaluation of the connection corrosion rate, frequency of inspection, and number of rivets that it has as for the tension only case.

Recommended Procedure for Evaluating a Riveted Connection

The engineers tasked with preparing plans and specifications for and supervising the construction of rehabilitation work will undoubtedly make decisions on the replacement of structural steel rivets. These decisions can affect the integrity of the structure being reconditioned as well as the cost of the work being performed.

Therefore, the formation of standard guidelines would be extremely beneficial to both the engineer doing the work and the organization that is paying for it.

The following recommended procedure is a general method which can be applied to any riveted structure:

1. Visually identify all connections containing rivets which show signs of significant corrosion.
2. Categorize each connection as the type which loads the rivets in one of the three possible modes (shear, tension, or combined shear and tension).
3. Clean the connections as much as reasonably possible and measure the amount of head deterioration. All headless and loose rivets shall be replaced with high-strength bolts regardless of connection type. A rivet shall be deemed loose if it can be felt to move after being struck on the side of the head in a direction approximately perpendicular to its shank with a 40 oz. engineer's hammer.
4. For shear connections, as long as there a partial lip beyond the rivet hole and the corrosion has not entered the shank, it need not be replaced.
5. For tension connections, the measured amount of head deterioration shall not exceed 35% of its total head volume. Application of this value shall take into consideration the corrosion rate of the connection, its frequency of inspection, and the number of rivets.

6. For connections subjected to combined shear and tension, a linear interaction between the percentage of force in tension and the amount of tolerable head deterioration (see Figure 16, page 36) shall be assumed. Application of the value determined shall also give due consideration to the corrosion rate of the connection, its frequency of inspection, and the number of rivets.

Future Work

Although the condition of uniform, symmetrical corrosion is the type most commonly found, there will also be situations where the rivet is subjected to one or more of the non-symmetrical, localized forms of corrosion described in Chapter II. As such, it is also necessary to investigate the behavior of these conditions to confidently prescribe allowable limits as was done for the symmetrical uniform and non-uniform cases. The work would have to be performed in 3-D to accurately model the unbalanced material loss and leads to large, complicated models.

With most finite element structural analysis problems, the geometry used can significantly affect the results obtained. The button head rivet, though the most commonly used rivet, is not the only type found. Future work should also investigate the effects of corrosion on the behavior of other head types (high button, cone, countersunk, oval countersunk, and pan) used.

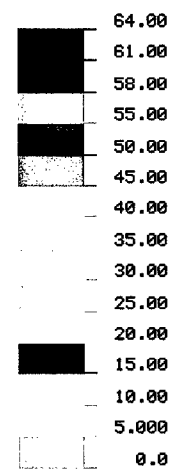
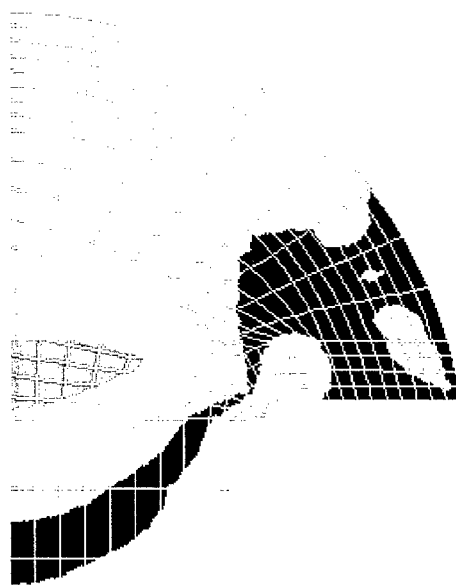
Further studies should also include physical testing of deteriorated rivets. One anticipates that this testing will correlate to and thus support the theoretical findings that have been presented.

APPENDIX A

UNIFORM MODEL STRESS CONTOURS

DISPLAY III - GEOMETRY MODELING SYSTEM (5.1.0) PRE/POST MODULE

VON-MISES STRESS

VIEW : 4.09031
RANGE: 37.38176

EMRC-NISA/DISPLAY

MAR/16/95 16:15:10

4Y
↑
ROT X 0.0
ROT Y 0.0
→ X ROT Z 0.0

EMRC

TIME: 0.10000E+01
0% DETERIORATION / UNIFORM PRESSURE

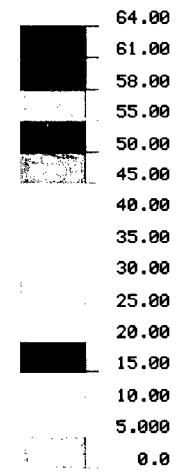
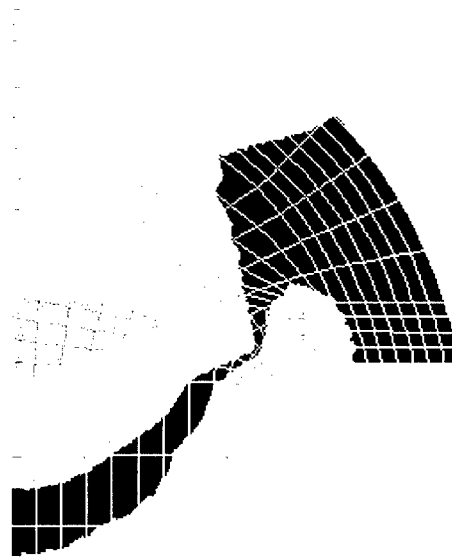
0% Stress Contours / Uniform Loss - Uniform Pressure

DISPLAY III - GEOMETRY MODELING SYSTEM (5.1.0) PRE/POST MODULE

VON-MISES STRESS

VIEW : 3.885144

RANGE: 37.61539



EMRC-NISA/DISPLAY

MAR/16/95 16:17:15

↑ Y ROTX
0.0
→ X ROTY
0.0
ROTZ
0.0

EMRC

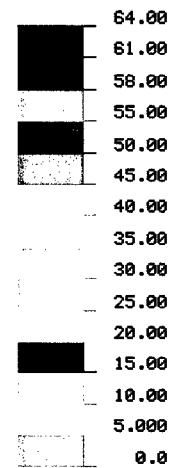
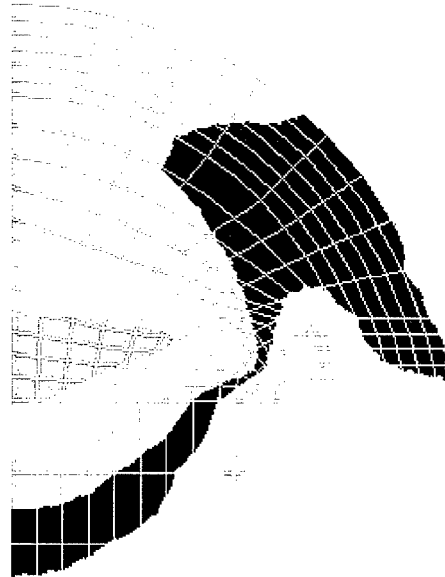
TIME: 0.10000E+01

10% DETERIORATION / UNIFORM PRESSURE

10% Stress Contours / Uniform Loss - Uniform Pressure

DISPLAY III - GEOMETRY MODELING SYSTEM (5.1.0) PRE/POST MODULE

VON-MISES STRESS

VIEW : 3.684731
RANGE: 38.81832TIME: 0.10000E+01
20% DETERIORATION / UNIFORM PRESSURE

EMRC-NISA/DISPLAY

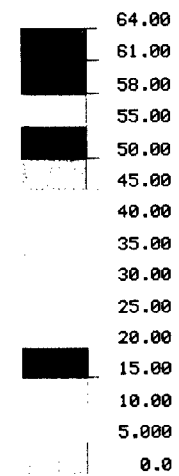
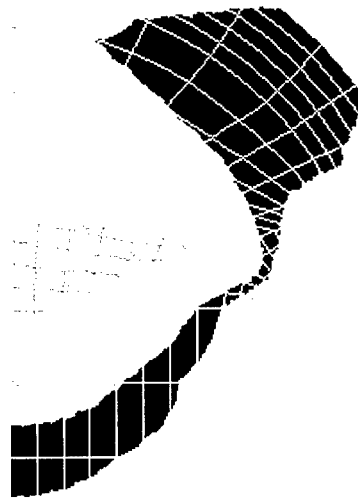
MAR/16/95 16:19:35

ROTX
0.0
ROTY
0.0
ROTZ
0.0

20% Stress Contours / Uniform Loss - Uniform Pressure

DISPLAY III - GEOMETRY MODELING SYSTEM (5.1.0) PRE/POST MODULE

VON-MISES STRESS

VIEW : 3.493001
RANGE: 38.23979

EMRC-NISA/DISPLAY

MAR/16/95 16:21:29

↑ Y ROTX
0.0
→ X ROTY
0.0
ROTZ
0.0

EM
RC

TIME: 0.10000E+01

30% DETERIORATION / UNIFORM PRESSURE

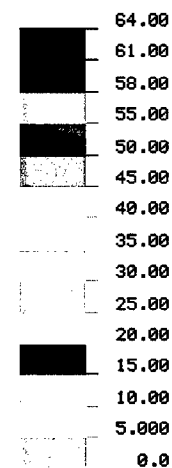
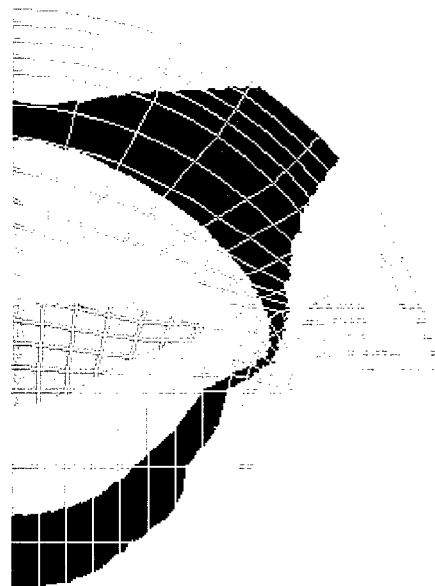
30% Stress Contours / Uniform Loss - Uniform Pressure

DISPLAY III - GEOMETRY MODELING SYSTEM (5.1.0) PRE/POST MODULE

VON-MISES STRESS

VIEW : 3.235777

RANGE: 38.493



EMRC-NISA/DISPLAY

MAR/16/95 16:23:39

Y
X
ROTX
0.0
ROTY
0.0
ROTZ
0.0

EM
RC

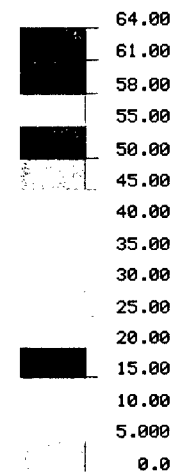
TIME: 0.10000E+01

40% DETERIORATION / UNIFORM PRESSURE

40% Stress Contours / Uniform Loss - Uniform Pressure

DISPLAY III - GEOMETRY MODELING SYSTEM (5.1.0) PRE/POST MODULE

VON-MISES STRESS

VIEW : 3.012618
RANGE: 39.35607

EMRC-NISA/DISPLAY

MAR/16/95 16:25:55

↑ Y ROTX
0.0
→ X ROTY
0.0
ROTZ
0.0

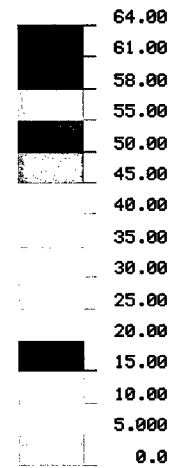
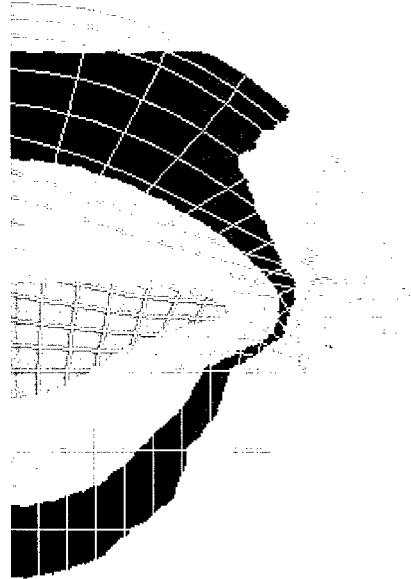
TIME: 0.10000E+01
UNIFORM PRESSURE / 50% DETERIORATION**50% Stress Contours / Uniform Loss - Uniform Pressure**

DISPLAY III - GEOMETRY MODELING SYSTEM (5.1.0) PRE/POST MODULE

VON-MISES STRESS

VIEW : 2.462215

RANGE: 47.73489



EMRC-NISA/DISPLAY

MAR/16/95 16:29:17

↑ Y
→ X
ROTX
0.0
ROTY
0.0
ROTZ
0.0



TIME: 0.10000E+01

UNIFORM PRESSURE / 60% DETERIORATION

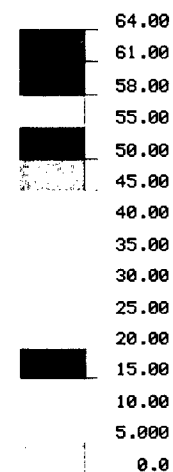
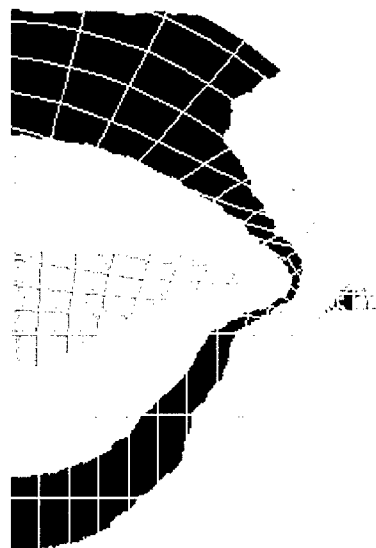
60% Stress Contours / Uniform Loss - Uniform Pressure

DISPLAY III - GEOMETRY MODELING SYSTEM (5.1.0) PRE/POST MODULE

VON-MISES STRESS

VIEW : 2.358106

RANGE: 60.79137



EMRC-NISA/DISPLAY

MAR/16/95 16:32:46

↑ Y
→ X
ROTX 0.0
ROTY 0.0
ROTZ 0.0



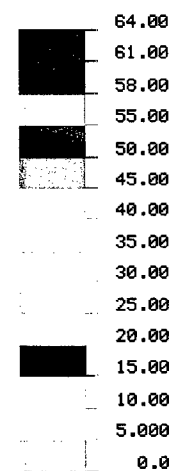
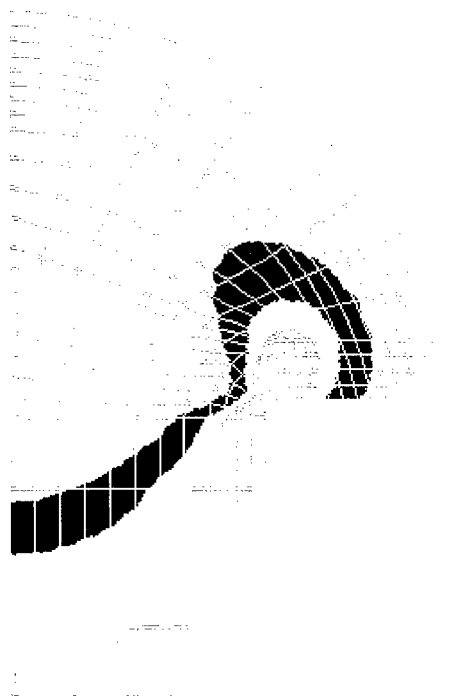
TIME: 0.10000E+01

UNIFORM PRESSURE / 70% DETERIORATION

70% Stress Contours / Uniform Loss - Uniform Pressure

DISPLAY III - GEOMETRY MODELING SYSTEM (5.1.0) PRE/POST MODULE

VON-MISES STRESS

VIEW : 4.9716
RANGE: 37.62475

EMRC-NISA/DISPLAY

MAR/16/95 16:35:17

↑ Y ROTX
0.0
→ X ROTY
0.0
ROTZ
0.0

EM
RC

TIME: 0.10000E+01

0% DETERIORATION / LINEARLY VARYING PRESSURE

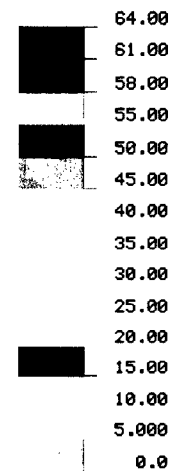
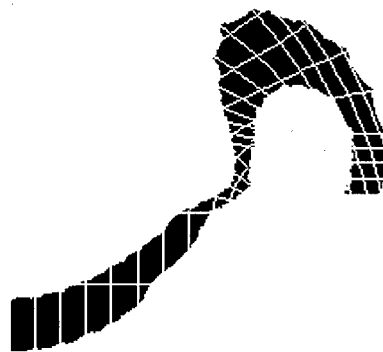
0% Stress Contours / Uniform Loss - Linearly Decreasing Pressure

DISPLAY III - GEOMETRY MODELING SYSTEM (5.1.0) PRE/POST MODULE

VON-MISES STRESS

VIEW : 5.645139

RANGE: 37.96785



EMRC-NISA/DISPLAY

MAR/16/95 16:38:20

↑ Y ROTX
0.0
→ X ROTY
0.0
ROTZ
0.0



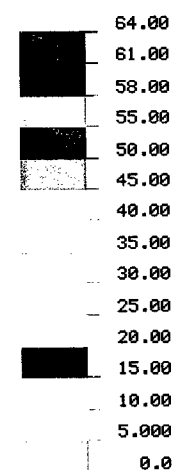
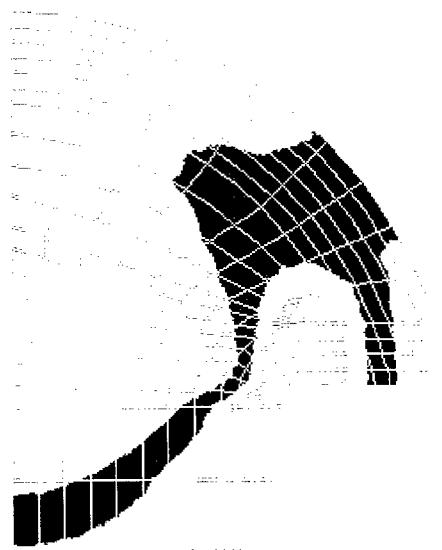
TIME: 0.10000E+01

10% DETERIORATION / LINEARLY VARYING PRESSURE

10% Stress Contours / Uniform Loss - Linearly Decreasing Pressure

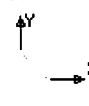
DISPLAY III - GEOMETRY MODELING SYSTEM (5.1.0) PRE/POST MODULE

VON-MISES STRESS

VIEW : 5.445143
RANGE: 38.67876

EMRC-NISA/DISPLAY

MAR/16/95 16:40:32



ROTX
0.0
ROTY
0.0
ROTZ
0.0

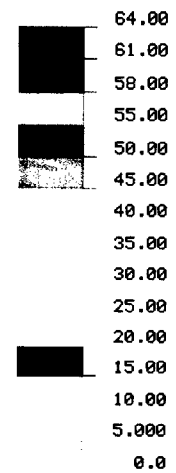
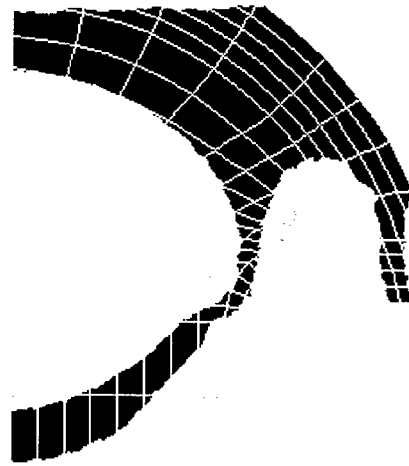
TIME: 0.10000E+01
20% DETERIORATION / LINEARLY VARYING PRESSURE**20% Stress Contours / Uniform Loss - Linearly Decreasing Pressure**

DISPLAY III - GEOMETRY MODELING SYSTEM (5.1.0) PRE/POST MODULE

VON-MISES STRESS

VIEW : 5.147581

RANGE: 39.56104



EMRC-NISA/DISPLAY

MAR/16/95 16:44:02

↑ Y ROTX
0.0
→ X ROTY
0.0
ROTZ
0.0

EMRC

TIME: 0.10000E+01

30% DETERIORATION / LINEARLY VARYING PRESSURE

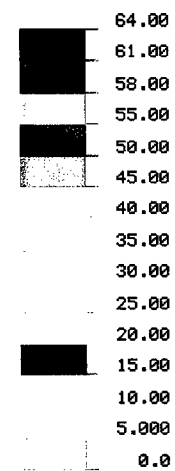
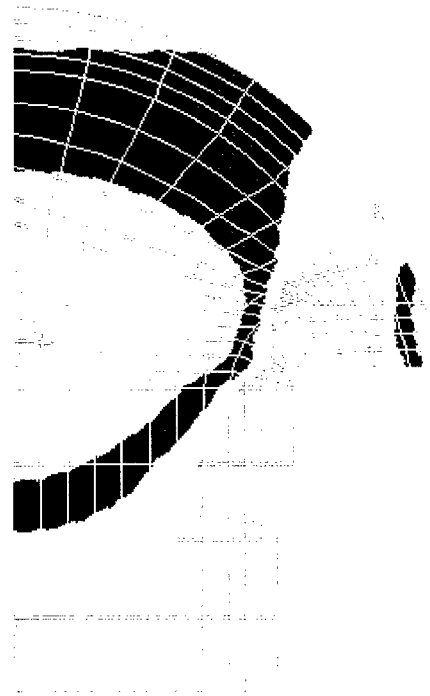
30% Stress Contours / Uniform Loss - Linearly Decreasing Pressure

DISPLAY III - GEOMETRY MODELING SYSTEM (5.1.0) PRE/POST MODULE

VON-MISES STRESS

VIEW : 4.798221

RANGE: 40.90509



EMRC-NISA/DISPLAY

MAR/16/95 16:48:16

↑ Y ROTX
0.0
→ X ROTY
0.0
ROTZ
0.0

EMRC

TIME: 0.10000E+01

40% DETERIORATION / LINEARLY VARYING PRESSURE

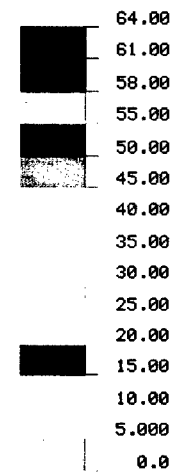
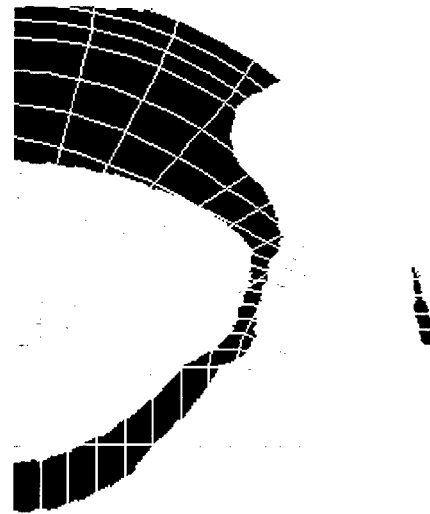
40% Stress Contours / Uniform Loss - Linearly Decreasing Pressure

DISPLAY III - GEOMETRY MODELING SYSTEM (5.1.0) PRE/POST MODULE

VON-MISES STRESS

VIEW : 4.472295

RANGE: 44.46076



EMRC-NISA/DISPLAY

MAR/16/95 16:50:29

↑ Y ROTX
0.0
→ X ROTY
0.0
ROTZ
0.0

EMRC

TIME: 0.10000E+01

50% DETERIORATION / LINEARLY VARYING PRESSURE

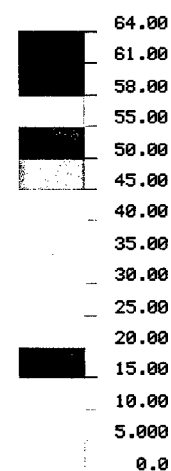
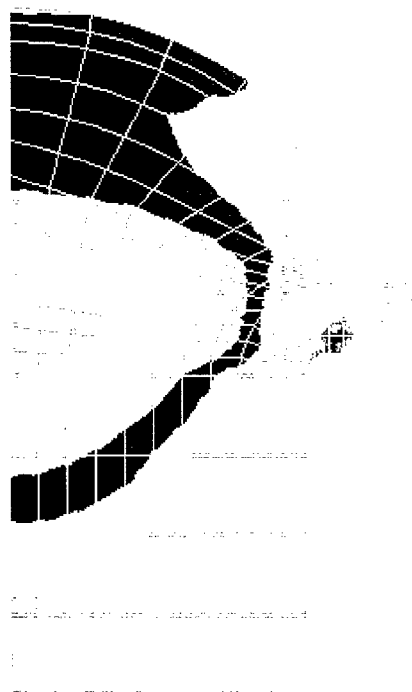
50% Stress Contours / Uniform Loss - Linearly Decreasing Pressure

DISPLAY III - GEOMETRY MODELING SYSTEM (5.1.0) PRE/POST MODULE

VON-MISES STRESS

VIEW : 4.193255

RANGE: 57.82307



EMRC-NISA/DISPLAY

MAR/16/95 16:52:33

4Y
X
ROTX
0.0
ROTY
0.0
ROTZ
0.0

EM
RC

TIME: 0.10000E+01

60% DETERIORATION / LINEARLY VARYING PRESSURE

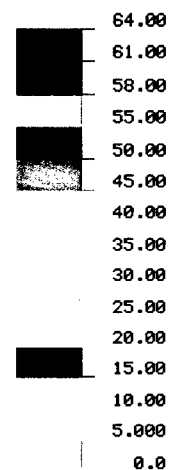
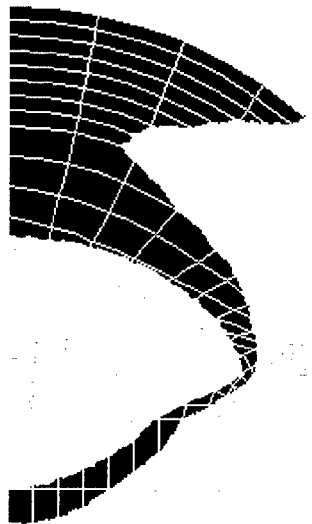
60% Stress Contours / Uniform Loss - Linearly Decreasing Pressure

DISPLAY III - GEOMETRY MODELING SYSTEM (5.1.0) PRE/POST MODULE

VON-MISES STRESS

VIEW : 3.266748

RANGE: 41.66653



EMRC-NISA/DISPLAY

MAR/16/95 16:54:51

↑ Y ROTX
0.0
→ X ROTY
0.0
ROTZ
0.0

EMRC

TIME: 0.10000E+01

0% DETERIORATION / LINEARLY VARYING PRESSURE

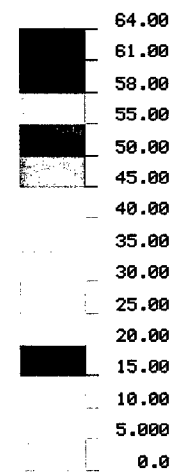
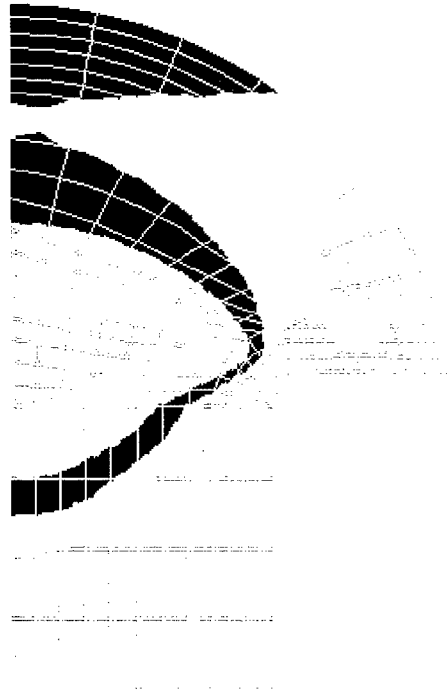
0% Stress Contours / Uniform Loss - Linearly Increasing Pressure

DISPLAY III - GEOMETRY MODELING SYSTEM (5.1.0) PRE/POST MODULE

VON-MISES STRESS

VIEW : 2.725346

RANGE: 42.085



EMRC-NISA/DISPLAY

MAR/16/95 16:56:54

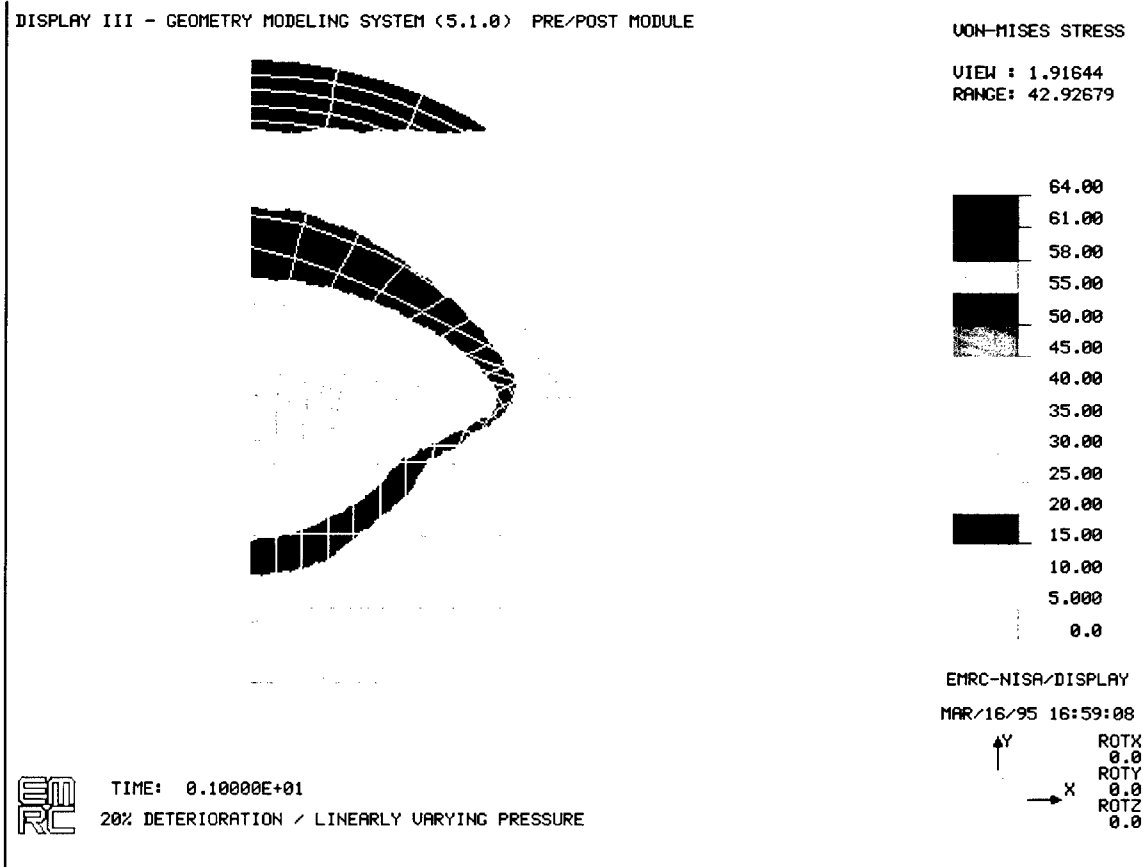
↑ Y ROTX
0.0
→ X ROTY
0.0
ROTZ
0.0

EM
RC

TIME: 0.10000E+01

10% DETERIORATION / LINEARLY VARYING PRESSURE

10% Stress Contours / Uniform Loss - Linearly Increasing Pressure

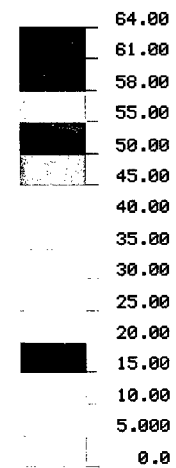
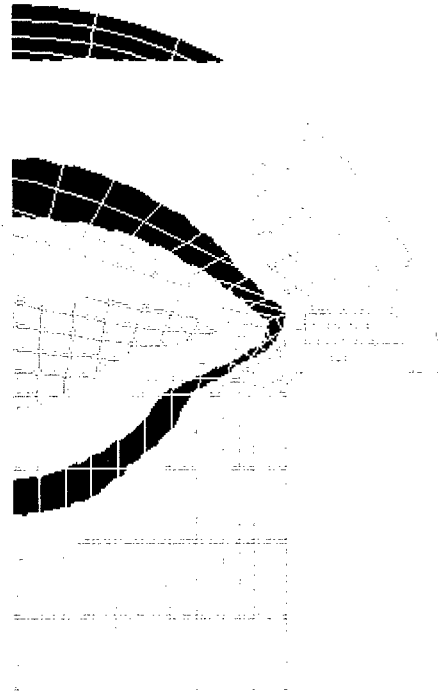


20% Stress Contours / Uniform Loss - Linearly Increasing Pressure

DISPLAY III - GEOMETRY MODELING SYSTEM (5.1.0) PRE/POST MODULE

VON-MISES STRESS

VIEW : 1.399114
RANGE: 43.82459



EMRC-NISA/DISPLAY

MAR/16/95 17:01:12

↑ Y ROTX 0.0
→ X ROTY 0.0
ROTZ 0.0

EMRC

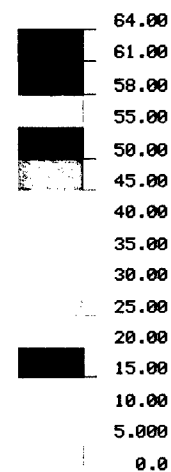
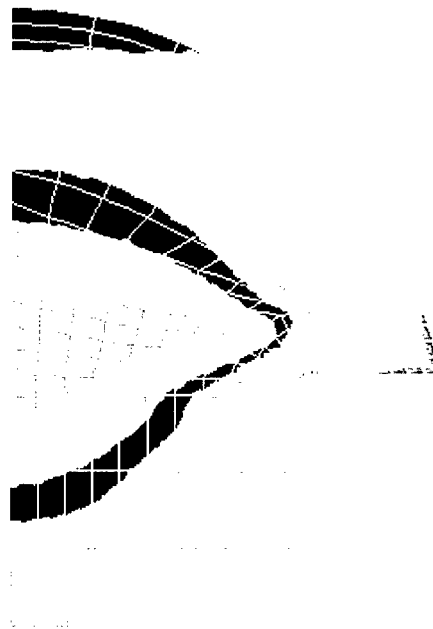
TIME: 0.10000E+01

30% DETERIORATION / LINEARLY VARYING PRESSURE

30% Stress Contours / Uniform Loss - Linearly Increasing Pressure

DISPLAY III - GEOMETRY MODELING SYSTEM (5.1.0) PRE/POST MODULE

VON-MISES STRESS

VIEW : 1.3189
RANGE : 49.49335

EMRC-NISA/DISPLAY

MAR/16/95 17:03:15

↑ Y ROTX
0.0
→ X ROTY
0.0
ROTZ
0.0

EMRC

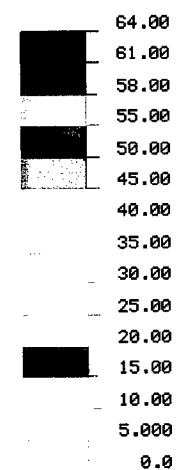
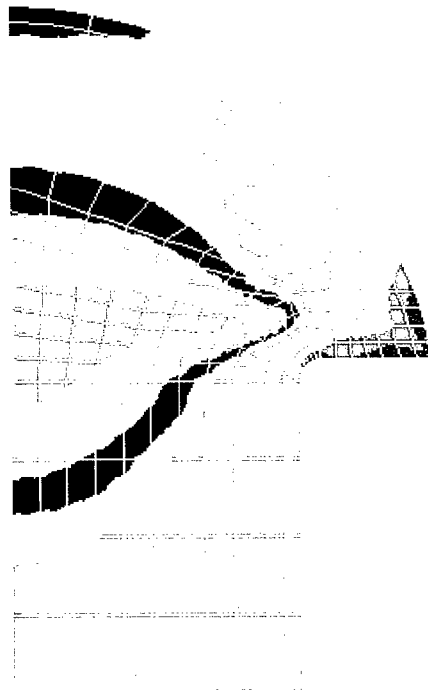
TIME: 0.10000E+01

40% DETERIORATION / LINEARLY VARYING PRESSURE

40% Stress Contours / Uniform Loss - Linearly Increasing Pressure

DISPLAY III - GEOMETRY MODELING SYSTEM (5.1.0) PRE/POST MODULE

VON-MISES STRESS

VIEW : 0.7844261
RANGE: 57.08339

EMRC-NISA/DISPLAY

MAR/16/95 17:05:16

ROTX
0.0
ROTY
0.0
ROTZ
0.0

EM
RC

TIME: 0.10000E+01

50% DETERIORATION / LINEARLY VARYING PRESSURE

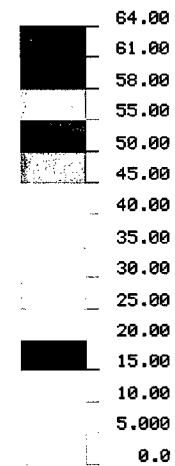
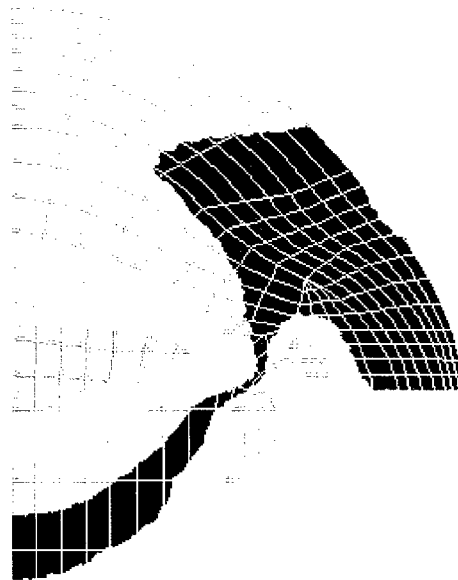
50% Stress Contours / Uniform Loss - Linearly Increasing Pressure

APPENDIX B

NON-UNIFORM MODEL STRESS CONTOURS

DISPLAY III - GEOMETRY MODELING SYSTEM (5.1.0) PRE/POST MODULE

VON-MISES STRESS

VIEW : 3.552036
RANGE: 39.39315

EMRC-NISA/DISPLAY

MAR/17/95 08:00:38

Y
↑
X
→

ROTX
0.0
ROTY
0.0
ROTZ
0.0



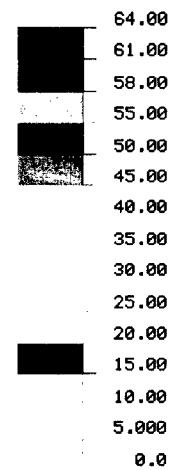
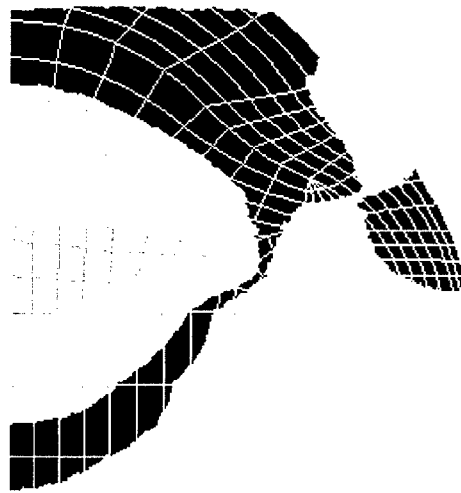
TIME: 0.10000E+01

7/8" BUTTON HEAD RIVET / 10% NON-UNIFORM DETERIORATION

10% Stress Contours / Non-Uniform Loss - Uniform Pressure

DISPLAY III - GEOMETRY MODELING SYSTEM (5.1.0) PRE/POST MODULE

VON-MISES STRESS

VIEW : 3.046659
RANGE: 39.89446

EMRC-NISA/DISPLAY

MAR/17/95 08:08:57

↑ Y ROTX
 ROTY
→ X ROTZ

EMRC

TIME: 0.10000E+01

7/8" BUTTON HEAD RIVET / 20% NON-UNIFORM DETERIORATION

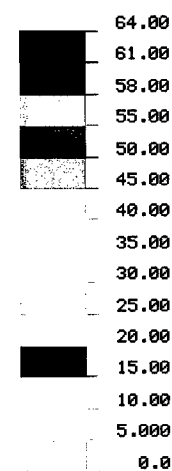
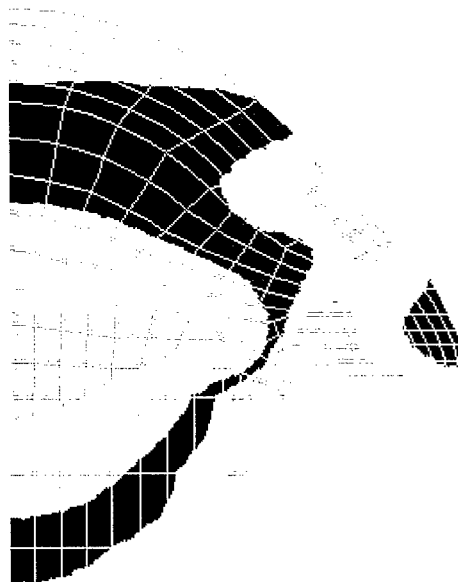
20% Stress Contours / Non-Uniform Loss - Uniform Pressure

DISPLAY III - GEOMETRY MODELING SYSTEM (5.1.0) PRE/POST MODULE

VON-MISES STRESS

VIEW : 2.524457

RANGE: 40.7572



EMRC-NISA/DISPLAY

MAR/17/95 08:12:03

↑ Y RDTX
0.0
→ X RDTY
0.0
RDTZ
0.0

EMRC

TIME: 0.10000E+01

7/8" BUTTON HEAD RIVET / 30% NON-UNIFORM DETERIORATION

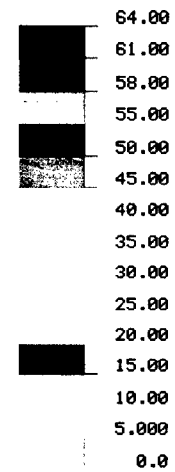
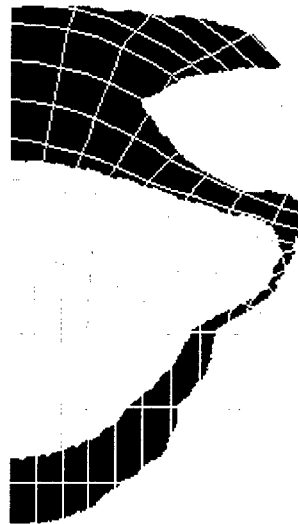
30% Stress Contours / Non-Uniform Loss - Uniform Pressure

DISPLAY III - GEOMETRY MODELING SYSTEM (5.1.0) PRE/POST MODULE

VON-MISES STRESS

VIEW : 2.044402

RANGE: 43.109



EMRC-NISA/DISPLAY

MAR/17/95 08:15:39

↑ Y ROTX
0.0
→ X ROTY
0.0
ROTZ
0.0

EMRC

TIME: 0.10000E+01

7/8" BUTTON HEAD RIVET / 40% NON-UNIFORM DETERIORATION

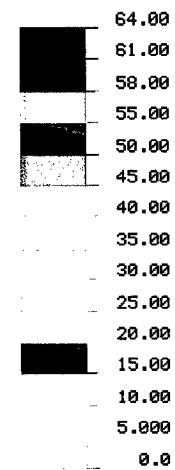
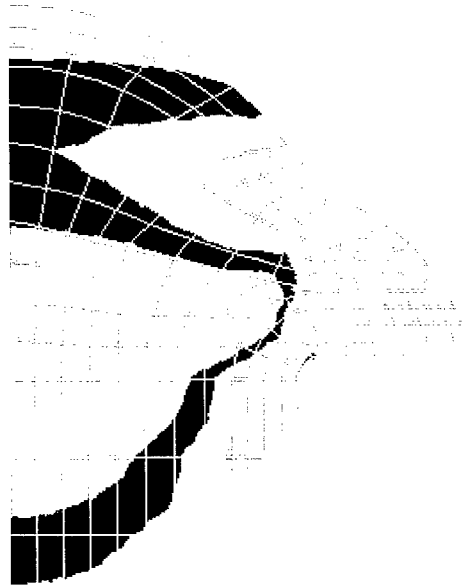
40% Stress Contours / Non-Uniform Loss - Uniform Pressure

DISPLAY III - GEOMETRY MODELING SYSTEM (5.1.0) PRE/POST MODULE

VON-MISES STRESS

VIEW : 1.540268

RANGE: 51.26744



EMRC-NISA/DISPLAY

MAR/17/95 08:17:48

↑ Y ROTX
0.0
→ X ROTY
0.0
ROTZ
0.0

EMRC

TIME: 0.10000E+01

7/8" BUTTON HEAD RIVET / 50% NON-UNIFORM DETERIORATION

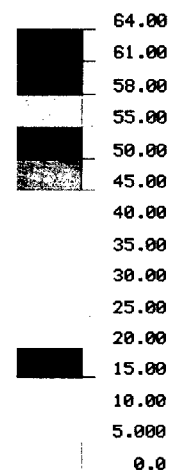
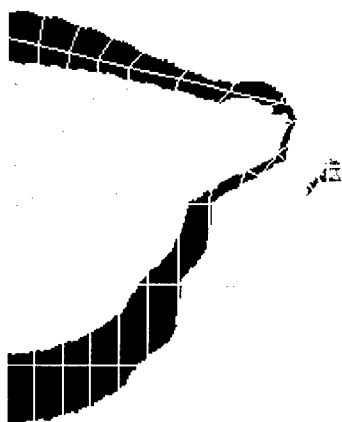
50% Stress Contours / Non-Uniform Loss - Uniform Pressure

DISPLAY III - GEOMETRY MODELING SYSTEM (5.1.0) PRE/POST MODULE

VON-MISES STRESS

VIEW : 0.4166785

RANGE: 61.95961



EMRC-NISA/DISPLAY

MAR/17/95 08:19:58

↑ Y ROTX
0.0
→ X ROTY
0.0
ROTZ
0.0

EMRC

TIME: 0.10000E+01

7/8" BUTTON HEAD RIVET / 60% NON-UNIFORM DETERIORATION

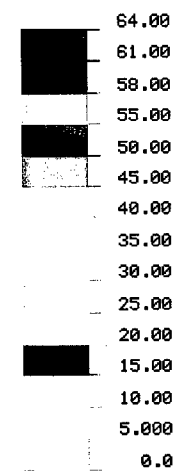
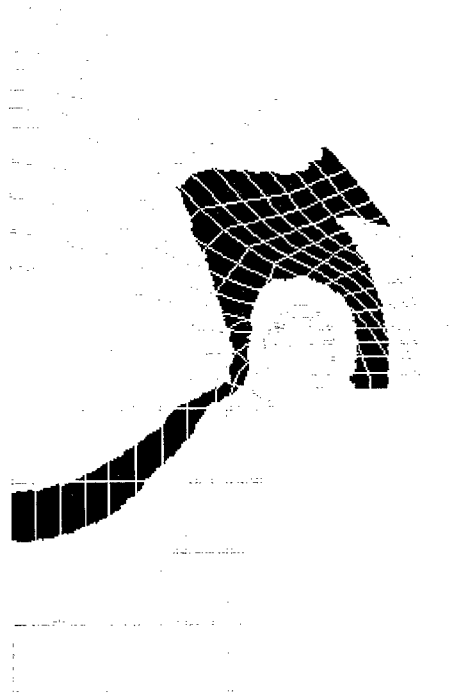
60% Stress Contours / Non-Uniform Loss - Uniform Pressure

DISPLAY III - GEOMETRY MODELING SYSTEM (5.1.0) PRE/POST MODULE

VON-MISES STRESS

VIEW : 5.005003

RANGE: 40.00903



EMRC-NISA/DISPLAY

MAR/17/95 08:23:06

ΔY ROTX
0.0
→ X ROTY
0.0
ROTZ
0.0

EM
RC

TIME: 0.10000E+01

7/8" BUTTON HEAD RIVET / 10% NON-UNIFORM DETERIORATION

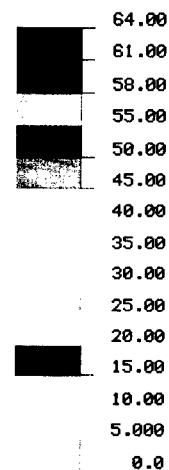
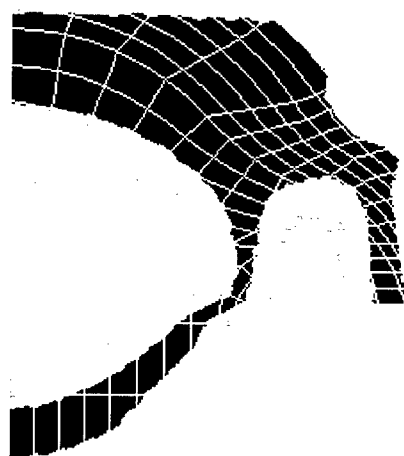
10% Stress Contours / Non-Uniform Loss - Linearly Decreasing Pressure

DISPLAY III - GEOMETRY MODELING SYSTEM (5.1.0) PRE/POST MODULE

VON-MISES STRESS

VIEW : 5.111271

RANGE: 40.49635



EMRC-NISA/DISPLAY

MAR/17/95 08:25:22

↑ Y ROTX
0.0
→ X ROTY
0.0
ROTZ
0.0

EM
RC

TIME: 0.10000E+01

7/8" BUTTON HEAD RIVET / 20% NON-UNIFORM DETERIORATION

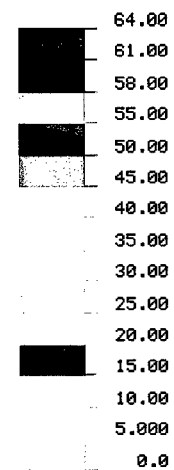
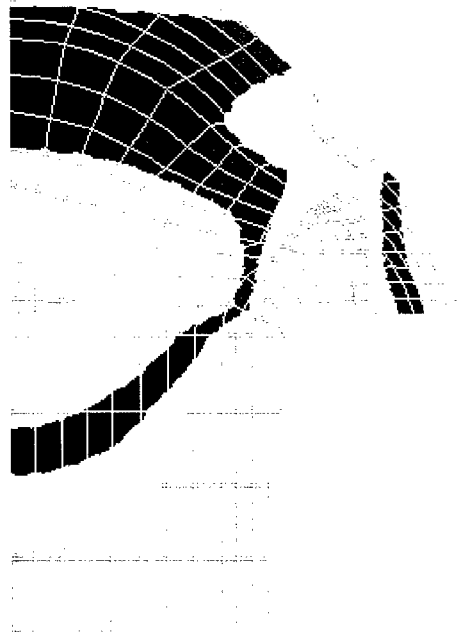
20% Stress Contours / Non-Uniform Loss - Linearly Decreasing Pressure

DISPLAY III - GEOMETRY MODELING SYSTEM (5.1.0) PRE/POST MODULE

VON-MISES STRESS

VIEW : 4.546164

RANGE: 41.4



EMRC-NISA/DISPLAY

MAR/17/95 08:27:32

↑ Y ROTX
0.0
→ X ROTY
0.0
ROTZ
0.0

EMRC

TIME: 0.10000E+01

7/8" BUTTON HEAD RIVET / 30% NON-UNIFORM DETERIORATION

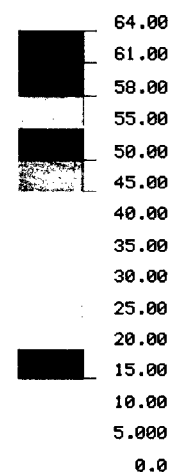
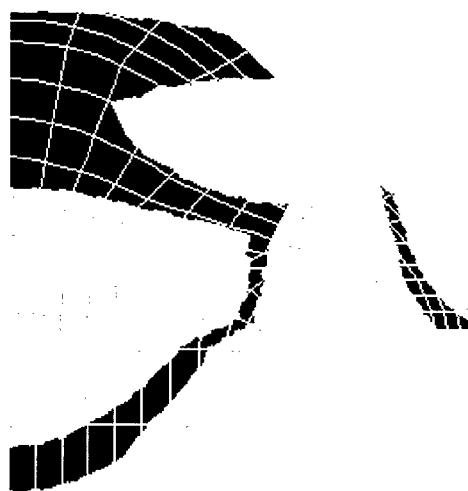
30% Stress Contours / Non-Uniform Loss - Linearly Decreasing Pressure

DISPLAY III - GEOMETRY MODELING SYSTEM (5.1.0) PRE/POST MODULE

VON-MISES STRESS

VIEW : 4.247008

RANGE: 47.20368



EMRC-NISA/DISPLAY

MAR/17/95 08:29:41

↑ Y ROTX
0.0
→ X ROTY
0.0
ROTZ
0.0

EMRC

TIME: 0.10000E+01

7/8" BUTTON HEAD RIVET / 40% NON-UNIFORM DETERIORATION

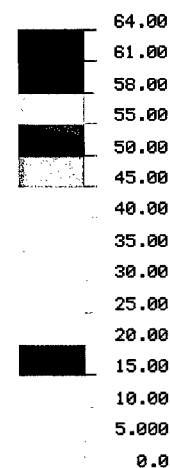
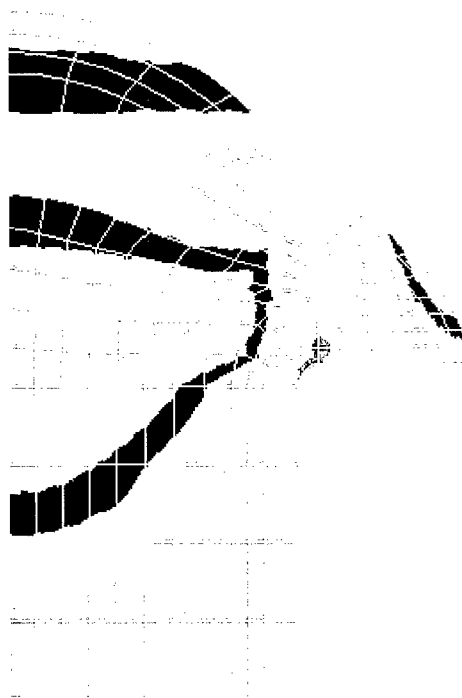
40% Stress Contours / Non-Uniform Loss - Linearly Decreasing Pressure

DISPLAY III - GEOMETRY MODELING SYSTEM (5.1.0) PRE/POST MODULE

VON-MISES STRESS

VIEW : 3.796801

RANGE: 57.49497



EMRC-NISA/DISPLAY

MAR/17/95 08:32:04

↑ Y ROTX
0.0
ROT Y
0.0
→ X ROT Z
0.0

EMRC

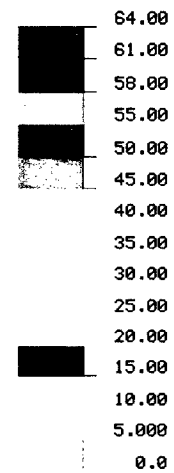
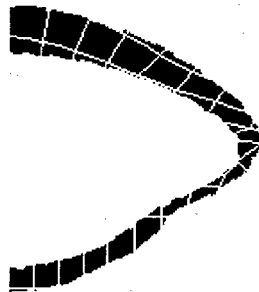
TIME: 0.10000E+01

7/8" BUTTON HEAD RIVET / 50% NON-UNIFORM DETERIORATION

50% Stress Contours / Non-Uniform Loss - Linearly Decreasing Pressure

DISPLAY III - GEOMETRY MODELING SYSTEM (5.1.0) PRE/POST MODULE

VON-MISES STRESS

VIEW : 2.478534
RANGE: 46.84366

EMRC-NISA/DISPLAY

MAR/17/95 08:35:36

↑ Y ROTX
0.0
→ X ROTY
0.0
ROTZ
0.0

EMRC

TIME: 0.10000E+01

7/8" BUTTON HEAD RIVET / 10% NON-UNIFORM DETERIORATION

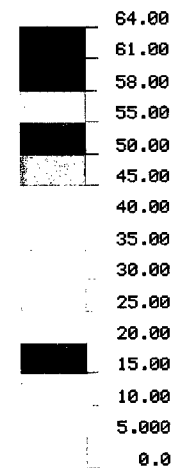
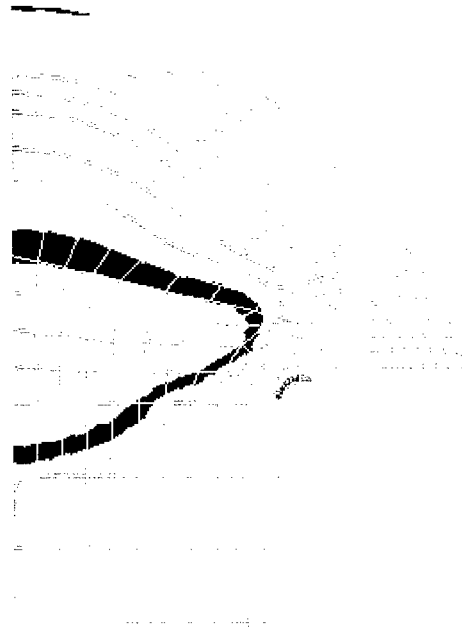
10% Stress Contours / Non-Uniform Loss - Linearly Increasing Pressure

DISPLAY III - GEOMETRY MODELING SYSTEM (5.1.0) PRE/POST MODULE

VON-MISES STRESS

VIEW : 2.235074

RANGE: 58.48326



EMRC-NISA/DISPLAY

MAR/17/95 08:39:09

↑ Y ROTX
 ROTY
 → X ROTZ
 0.0

EMRC

TIME: 0.10000E+01

7/8" BUTTON HEAD RIVET / 20% NON-UNIFORM DETERIORATION

20% Stress Contours / Non-Uniform Loss - Linearly Increasing Pressure

REFERENCES

- [1] American Institute of Steel Construction, Inc. 1989. Manual of Steel Construction - Allowable Stress Design. Chicago, Ill.
- [2] American Society for Testing and Materials. 1993. Steel Structural Rivets. Designation: ASTM A502-93. Philadelphia, Pa.
- [3] Bennett, P.A. 1983. "From Wire to Rivets." Wire Journal International, November.
- [4] Bower, J.E., M.R. Kaczinske, Z. Ma, Y. Zhou, J.D. Wood, and B.T. Yen. 1994. Structural Evaluation of Riveted Spillway Gates. Washington, D.C.: U.S. Army Corps of Engineers. Technical Report REMR-CS-43.
- [5] Engineering Mechanics Research Corporation. 1992. DISPLAY III User's Manual 1. Troy, Mich.
- [6] Engineering Mechanics Research Corporation. 1992. NISA II User's Manual. Troy, Mich.
- [7] Fazio, A.E., and R.N Fazio. 1984. "Rivet Replacement criteria." Second Bridge Engineering Conference. Washington, D.C. Transportation Research Board. Vol 1, TRR 950.
- [8] Fisher, J., and J. Struik. 1974. Guide to Design Criteria for Bolted and Riveted Joints. New York, N.Y.: John Wiley & Sons.
- [9] Fontana, M.G., and N.D. Greene. 1967. Corrosion Engineering. New York, N.Y.: McGraw-Hill.
- [10] Henthorne, M. 1971. Fundamentals of Corrosion. Chemical Engineering reprint, McGraw-Hill, Inc., New York, N.Y.
- [11] Johnson, J.E., and C.G. Salmon. 1980. Steel Structures: Design and Behavior. New York, N.Y.: Harper and Row.
- [12] Johnston, P.R., and W. Weaver. 1984. Finite Elements for Structural Analysis. Englewood Cliffs, N.J.: Prentice-Hall.

- [13] McCormac, J.C. 1971. Structural Steel Design. New York, N.Y.: Intext Educational.
- [14] Munse, W.H. 1976. "Fifty Years of Riveted, Bolted, and Welded Steel Construction." Journal of the Construction Division, September.
- [15] Oliver, W.A., and W.M. Wilson. 1930. Tension Tests of Rivets. University of Illinois Experiment Station Bulletin 210. Urbana, Ill.
- [16] "Riveting Experience." Modern Steel Construction, September 1993.
- [17] The American Society of Mechanical Engineers. 1972. American National Standard, Large Rivets. Designation: ANSI B18.1.2 - 1972. New York, N.Y.
- [18] Uhlig, H.H. 1963. Corrosion and Corrosion Control. New York, N.Y.: John Wiley and Sons.

REPORT DOCUMENTATION PAGE

Form Approved
OMB No. 0704-0188

Public reporting burden for this collection of information is estimated to average 1 hour per response, including the time for reviewing instructions, searching existing data sources, gathering and maintaining the data needed, and completing and reviewing the collection of information. Send comments regarding this burden estimate or any other aspect of this collection of information, including suggestions for reducing this burden, to Washington Headquarters Services, Directorate for Information Operations and Reports, 1215 Jefferson Davis Highway, Suite 1204, Arlington, VA 22202-4302, and to the Office of Management and Budget, Paperwork Reduction Project (0704-0188), Washington, DC 20503.

1. AGENCY USE ONLY (Leave blank)		2. REPORT DATE December 1999	3. REPORT TYPE AND DATES COVERED Final report	
4. TITLE AND SUBTITLE Rivet Replacement Analysis			5. FUNDING NUMBERS	
6. AUTHOR(S) Erich Edward Reichle				
7. PERFORMING ORGANIZATION NAME(S) AND ADDRESS(ES) U.S. Army Engineer District, Jacksonville 400 W. Bay St. P.O. Box 4970 Jacksonville, FL 32202			8. PERFORMING ORGANIZATION REPORT NUMBER	
9. SPONSORING/MONITORING AGENCY NAME(S) AND ADDRESS(ES) U.S. Army Engineer Research and Development Center Information Technology Laboratory 3909 Halls Ferry Road, Vicksburg, MS 39180-6199 U.S. Army Corps of Engineers Washington, DC 20314-1000			10. SPONSORING/MONITORING AGENCY REPORT NUMBER Technical Report ITL-99-5	
11. SUPPLEMENTARY NOTES				
12a. DISTRIBUTION/AVAILABILITY STATEMENT Approved for public release; distribution is unlimited.			12b. DISTRIBUTION CODE	
13. ABSTRACT (Maximum 200 words) <p>Recently there has been much discussion concerning deterioration of the infrastructure in the United States. Associated with this concern is the decay of structures built with steel some 30 to 40 years ago. Examples are numerous and include bridges on our highways, school and office buildings, and hydraulic structures used in flood control and water supply, just to name a few.</p> <p>An integral part of each of these structures is their connections. Since riveted connections were widely used, there is particular interest in material loss due to corrosion in rivets and its effect on connection performance. Currently there is very limited information available to evaluate these effects and determine the structural integrity of the connection.</p> <p>This research is directed at developing criteria to determine when a corroded rivet should be replaced. This research develops numerical modeling to simulate the deterioration of a rivet. This model incorporates the stress that is developed from service loading.</p> <p>A two-dimensional axisymmetric model is developed using a numerically integrated finite element analysis computer program. Service loads are applied to determine the state of stress within the rivet. Elements modeling the rivet head are then made inactive to stimulate the corrosion process. Additional analyses are performed incrementally reducing the number of</p> <p style="text-align: right;">(Continued)</p>				
14. SUBJECT TERMS Corrosion Replacement Rivets Finite element analysis Riveted connections			15. NUMBER OF PAGES 89	
			16. PRICE CODE	
17. SECURITY CLASSIFICATION OF REPORT UNCLASSIFIED	18. SECURITY CLASSIFICATION OF THIS PAGE UNCLASSIFIED	19. SECURITY CLASSIFICATION OF ABSTRACT	20. LIMITATION OF ABSTRACT	

13. (Concluded).

elements modeling the rivet head to provide sufficient data to plot stress variations versus reduction of head area. This plot is used to identify a material loss threshold that may exist and its effect on rivet stability. In addition, it is proposed that this research be used to determine how much rivet head material can be lost before the rivet must be replaced.

REPORTS PUBLISHED UNDER THE COMPUTER-AIDED STRUCTURAL ENGINEERING (CASE) PROJECT

	Title	Date
Technical Report K-78-1	List of Computer Programs for Computer-Aided Structural Engineering	Feb 1978
Instruction Report O-79-2	User's Guide: Computer Program with Interactive Graphics for Analysis of Plane Frame Structures (CFRAME)	Mar 1979
Technical Report K-80-1	Survey of Bridge-Oriented Design Software	Jan 1980
Technical Report K-80-2	Evaluation of Computer Programs for the Design/Analysis of Highway and Railway Bridges	Jan 1980
Instruction Report K-80-1	User's Guide: Computer Program for Design/Review of Curvilinear Conduits/Culverts (CURCON)	Feb 1980
Instruction Report K-80-3	A Three-Dimensional Finite Element Data Edit Program	Mar 1980
Instruction Report K-80-4	A Three-Dimensional Stability Analysis/Design Program (3DSAD)	
	Report 1: General Geometry Module	Jun 1980
	Report 3: General Analysis Module (CGAM)	Jun 1982
	Report 4: Special-Purpose Modules for Dams (CDAMS)	Aug 1983
Instruction Report K-80-6	Basic User's Guide: Computer Program for Design and Analysis of Inverted-T Retaining Walls and Floodwalls (TWDA)	Dec 1980
Instruction Report K-80-7	User's Reference Manual: Computer Program for Design and Analysis of Inverted-T Retaining Walls and Floodwalls (TWDA)	Dec 1980
Technical Report K-80-4	Documentation of Finite Element Analyses	
	Report 1: Longview Outlet Works Conduit	Dec 1980
	Report 2: Anchored Wall Monolith, Bay Springs Lock	Dec 1980
Technical Report K-80-5	Basic Pile Group Behavior	Dec 1980
Instruction Report K-81-2	User's Guide: Computer Program for Design and Analysis of Sheet Pile Walls by Classical Methods (CSHTWAL)	
	Report 1: Computational Processes	Feb 1981
	Report 2: Interactive Graphics Options	Mar 1981
Instruction Report K-81-3	Validation Report: Computer Program for Design and Analysis of Inverted-T Retaining Walls and Floodwalls (TWDA)	Feb 1981
Instruction Report K-81-4	User's Guide: Computer Program for Design and Analysis of Cast-in-Place Tunnel Linings (NEWTUN)	Mar 1981
Instruction Report K-81-6	User's Guide: Computer Program for Optimum Nonlinear Dynamic Design of Reinforced Concrete Slabs Under Blast Loading (CBARCS)	Mar 1981
Instruction Report K-81-7	User's Guide: Computer Program for Design or Investigation of Orthogonal Culverts (CORTCUL)	Mar 1981
Instruction Report K-81-9	User's Guide: Computer Program for Three-Dimensional Analysis of Building Systems (CTABS80)	Aug 1981
Technical Report K-81-2	Theoretical Basis for CTABS80: A Computer Program for Three-Dimensional Analysis of Building Systems	Sep 1981
Instruction Report K-82-6	User's Guide: Computer Program for Analysis of Beam-Column Structures with Nonlinear Supports (CBEAMC)	Jun 1982

(Continued)

REPORTS PUBLISHED UNDER THE COMPUTER-AIDED STRUCTURAL ENGINEERING (CASE) PROJECT

(Continued)

	Title	Date
Instruction Report K-82-7	User's Guide: Computer Program for Bearing Capacity Analysis of Shallow Foundations (CBEAR)	Jun 1982
Instruction Report K-83-1	User's Guide: Computer Program with Interactive Graphics for Analysis of Plane Frame Structures (CFRAME)	Jan 1983
Instruction Report K-83-2	User's Guide: Computer Program for Generation of Engineering Geometry (SKETCH)	Jun 1983
Instruction Report K-83-5	User's Guide: Computer Program to Calculate Shear, Moment, and Thrust (CSMT) from Stress Results of a Two-Dimensional Finite Element Analysis	Jul 1983
Technical Report K-83-1	Basic Pile Group Behavior	Sep 1983
Technical Report K-83-3	Reference Manual: Computer Graphics Program for Generation of Engineering Geometry (SKETCH)	Sep 1983
Technical Report K-83-4	Case Study of Six Major General-Purpose Finite Element Programs	Oct 1983
Instruction Report K-84-2	User's Guide: Computer Program for Optimum Dynamic Design of Nonlinear Metal Plates Under Blast Loading (CSDOOR)	Jan 1984
Instruction Report K-84-7	User's Guide: Computer Program for Determining Induced Stresses and Consolidation Settlements (CSETT)	Aug 1984
Instruction Report K-84-8	Seepage Analysis of Confined Flow Problems by the Method of Fragments (CFRAG)	Sep 1984
Instruction Report K-84-11	User's Guide for Computer Program CGFAG, Concrete General Flexure Analysis with Graphics	Sep 1984
Technical Report K-84-3	Computer-Aided Drafting and Design for Corps Structural Engineers	Oct 1984
Technical Report ATC-86-5	Decision Logic Table Formulation of ACI 318-77, Building Code Requirements for Reinforced Concrete for Automated Constraint Processing, Volumes I and II	Jun 1986
Technical Report ITL-87-2	A Case Committee Study of Finite Element Analysis of Concrete Flat Slabs	Jan 1987
Instruction Report ITL-87-1	User's Guide: Computer Program for Two-Dimensional Analysis of U-Frame Structures (CUFRAM)	Apr 1987
Instruction Report ITL-87-2	User's Guide: For Concrete Strength Investigation and Design (CASTR) in Accordance with ACI 318-83	May 1987
Technical Report ITL-87-6	Finite-Element Method Package for Solving Steady-State Seepage Problems	May 1987
Instruction Report ITL-87-3	User's Guide: A Three-Dimensional Stability Analysis/Design Program (3DSAD) Module	Jun 1987
	Report 1: Revision 1: General Geometry	Jun 1987
	Report 2: General Loads Module	Sep 1989
	Report 6: Free-Body Module	Sep 1989

(Continued)

REPORTS PUBLISHED UNDER THE COMPUTER-AIDED STRUCTURAL ENGINEERING (CASE) PROJECT

(Continued)

	Title	Date
Instruction Report ITL-87-4	User's Guide: 2-D Frame Analysis Link Program (LINK2D)	Jun 1987
Technical Report ITL-87-4	Finite Element Studies of a Horizontally Framed Miter Gate Report 1: Initial and Refined Finite Element Models (Phases A, B, and C), Volumes I and II Report 2: Simplified Frame Model (Phase D) Report 3: Alternate Configuration Miter Gate Finite Element Studies--Open Section Report 4: Alternate Configuration Miter Gate Finite Element Studies--Closed Sections Report 5: Alternate Configuration Miter Gate Finite Element Studies--Additional Closed Sections Report 6: Elastic Buckling of Girders in Horizontally Framed Miter Gates Report 7: Application and Summary	Aug 1987
Instruction Report GL-87-1	User's Guide: UTEXAS2 Slope-Stability Package; Volume I, User's Manual	Aug 1987
Instruction Report ITL-87-5	Sliding Stability of Concrete Structures (CSLIDE)	Oct 1987
Instruction Report ITL-87-6	Criteria Specifications for and Validation of a Computer Program for the Design or Investigation of Horizontally Framed Miter Gates (CMITER)	Dec 1987
Technical Report ITL-87-8	Procedure for Static Analysis of Gravity Dams Using the Finite Element Method -- Phase 1a	Jan 1988
Instruction Report ITL-88-1	User's Guide: Computer Program for Analysis of Planar Grid Structures (CGRID)	Feb 1988
Technical Report ITL-88-1	Development of Design Formulas for Ribbed Mat Foundations on Expansive Soils	Apr 1988
Technical Report ITL-88-2	User's Guide: Pile Group Graphics Display (CPGG) Post-processor to CPGA Program	Apr 1988
Instruction Report ITL-88-2	User's Guide for Design and Investigation of Horizontally Framed Miter Gates (CMITER)	Jun 1988
Instruction Report ITL-88-4	User's Guide for Revised Computer Program to Calculate Shear, Moment, and Thrust (CSMT)	Sep 1988
Instruction Report GL-87-1	User's Guide: UTEXAS2 Slope-Stability Package; Volume II, Theory	Feb 1989
Technical Report ITL-89-3	User's Guide: Pile Group Analysis (CPGA) Computer Group	Jul 1989
Technical Report ITL-89-4	CBASIN--Structural Design of Saint Anthony Falls Stilling Basins According to Corps of Engineers Criteria for Hydraulic Structures; Computer Program X0098	Aug 1989

(Continued)

REPORTS PUBLISHED UNDER THE COMPUTER-AIDED STRUCTURAL ENGINEERING (CASE) PROJECT

(Continued)

	Title	Date
Technical Report ITL-89-5	CCHAN—Structural Design of Rectangular Channels According to Corps of Engineers Criteria for Hydraulic Structures; Computer Program X0097	Aug 1989
Technical Report ITL-89-6	The Response-Spectrum Dynamic Analysis of Gravity Dams Using the Finite Element Method; Phase II	Aug 1989
Contract Report ITL-89-1	State of the Art on Expert Systems Applications in Design, Construction, and Maintenance of Structures	Sep 1989
Instruction Report ITL-90-1	User's Guide: Computer Program for Design and Analysis of Sheet Pile Walls by Classical Methods (CWALSHT)	Feb 1990
Technical Report ITL-90-3	Investigation and Design of U-Frame Structures Using Program CUFRBC Volume A: Program Criteria and Documentation Volume B: User's Guide for Basins Volume C: User's Guide for Channels	May 1990
Instruction Report ITL-90-6	User's Guide: Computer Program for Two-Dimensional Analysis of U-Frame or W-Frame Structures (CWFRAM)	Sep 1990
Instruction Report ITL-90-2	User's Guide: Pile Group—Concrete Pile Analysis Program (CPGC) Preprocessor to CPGA Program	Jun 1990
Technical Report ITL-91-3	Application of Finite Element, Grid Generation, and Scientific Visualization Techniques to 2-D and 3-D Seepage and Groundwater Modeling	Sep 1990
Instruction Report ITL-91-1	User's Guide: Computer Program for Design and Analysis of Sheet-Pile Walls by Classical Methods (CWALSHT) Including Rowe's Moment Reduction	Oct 1991
Instruction Report ITL-87-2 (Revised)	User's Guide for Concrete Strength Investigation and Design (CASTR) in Accordance with ACI 318-89	Mar 1992
Technical Report ITL-92-2	Finite Element Modeling of Welded Thick Plates for Bonneville Navigation Lock	May 1992
Technical Report ITL-92-4	Introduction to the Computation of Response Spectrum for Earthquake Loading	Jun 1992
Instruction Report ITL-92-3	Concept Design Example, Computer-Aided Structural Modeling (CASM) Report 1: Scheme A Report 2: Scheme B Report 3: Scheme C	Jun 1992 Jun 1992 Jun 1992
Instruction Report ITL-92-4	User's Guide: Computer-Aided Structural Modeling (CASM) -Version 3.00	Apr 1992
Instruction Report ITL-92-5	Tutorial Guide: Computer-Aided Structural Modeling (CASM) -Version 3.00	Apr 1992

(Continued)

REPORTS PUBLISHED UNDER THE COMPUTER-AIDED STRUCTURAL ENGINEERING (CASE) PROJECT

(Continued)

	Title	Date
Contract Report ITL-92-1	Optimization of Steel Pile Foundations Using Optimality Criteria	Jun 1992
Technical Report ITL-92-7	Refined Stress Analysis of Melvin Price Locks and Dam	Sep 1992
Contract Report ITL-92-2	Knowledge-Based Expert System for Selection and Design of Retaining Structures	Sep 1992
Contract Report ITL-92-3	Evaluation of Thermal and Incremental Construction Effects for Monoliths AL-3 and AL-5 of the Melvin Price Locks and Dam	Sep 1992
Instruction Report GL-87-1	User's Guide: UTEXAS3 Slope-Stability Package; Volume IV, User's Manual	Nov 1992
Technical Report ITL-92-11	The Seismic Design of Waterfront Retaining Structures	Nov 1992
Technical Report ITL-92-12	Computer-Aided, Field-Verified Structural Evaluation	
	Report 1: Development of Computer Modeling Techniques for Miter Lock Gates	Nov 1992
	Report 2: Field Test and Analysis Correlation at John Hollis Bankhead Lock and Dam	Dec 1992
	Report 3: Field Test and Analysis Correlation of a Vertically Framed Miter Gate at Emsworth Lock and Dam	Dec 1993
Instruction Report GL-87-1	User's Guide: UTEXAS3 Slope-Stability Package; Volume III, Example Problems	Dec 1992
Technical Report ITL-93-1	Theoretical Manual for Analysis of Arch Dams	Jul 1993
Technical Report ITL-93-2	Steel Structures for Civil Works, General Considerations for Design and Rehabilitation	Aug 1993
Technical Report ITL-93-3	Soil-Structure Interaction Study of Red River Lock and Dam No. 1 Subjected to Sediment Loading	Sep 1993
Instruction Report ITL-93-3	User's Manual—ADAP, Graphics-Based Dam Analysis Program	Aug 1993
Instruction Report ITL-93-4	Load and Resistance Factor Design for Steel Miter Gates	Oct 1993
Technical Report ITL-94-2	User's Guide for the Incremental Construction, Soil-Structure Interaction Program SOILSTRUCT with Far-Field Boundary Elements	Mar 1994
Instruction Report ITL-94-1	Tutorial Guide: Computer-Aided Structural Modeling (CASM); Version 5.00	Apr 1994
Instruction Report ITL-94-2	User's Guide: Computer-Aided Structural Modeling (CASM); Version 5.00	Apr 1994
Technical Report ITL-94-4	Dynamics of Intake Towers and Other MDOF Structures Under Earthquake Loads: A Computer-Aided Approach	Jul 1994
Technical Report ITL-94-5	Procedure for Static Analysis of Gravity Dams Including Foundation Effects Using the Finite Element Method – Phase 1B	Jul 1994

(Continued)

REPORTS PUBLISHED UNDER THE COMPUTER-AIDED STRUCTURAL ENGINEERING (CASE) PROJECT

(Concluded)

	Title	Date
Instruction Report ITL-94-5	User's Guide: Computer Program for Winkler Soil-Structure Interaction Analysis of Sheet-Pile Walls (CWALSSI)	Nov 1994
Instruction Report ITL-94-6	User's Guide: Computer Program for Analysis of Beam-Column Structures with Nonlinear Supports (CBEAMC)	Nov 1994
Instruction Report ITL-94-7	User's Guide to CTWALL – A Microcomputer Program for the Analysis of Retaining and Flood Walls	Dec 1994
Contract Report ITL-95-1	Comparison of Barge Impact Experimental and Finite Element Results for the Lower Miter Gate of Lock and Dam 26	Jun 1995
Technical Report ITL-95-5	Soil-Structure Interaction Parameters for Structured/Cemented Silts	Aug 1995
Instruction Report ITL-95-1	User's Guide: Computer Program for the Design and Investigation of Horizontally Framed Miter Gates Using the Load and Resistance Factor Criteria (CMITER-LRFD)	Aug 1995
Technical Report ITL-95-8	Constitutive Modeling of Concrete for Massive Concrete Structures, A Simplified Overview	Sep 1995
Instruction Report ITL-96-1	User's Guide: Computer Program for Two-Dimensional Dynamic Analysis of U-Frame or W-Frame Structures (CDWFRM)	Jun 1996
Instruction Report ITL-96-2	Computer-Aided Structural Modeling (CASM), Version 6.00 Report 1: Tutorial Guide Report 2: User's Guide Report 3: Scheme A Report 4: Scheme B Report 5: Scheme C	Jun 1996
Technical Report ITL-96-8	Hyperbolic Stress-Strain Parameters for Structured/Cemented Silts	Aug 1996
Instruction Report ITL-96-3	User's Guide: Computer Program for the Design and Investigation of Horizontally Framed Miter Gates Using the Load and Resistance Factor Criteria (CMITERW-LRFD) Windows Version	Sep 1996
Instruction Report ITL-97-1	User's Guide: Computer Aided Inspection Forms for Hydraulic Steel Structures (CAIF-HSS), Windows Version	Sep 1997
Instruction Report ITL-97-2	User's Guide: Arch Dam Stress Analysis System (ADSAS)	Aug 1997
Instruction Report ITL-98-1	User's Guide for the Three-Dimensional Stability Analysis/Design (3DSAD) Program	Sep 1998
Technical Report ITL-98-4	Investigation of At-Rest Soil Pressures due to Irregular Sloping Soil Surfaces and CSOILP User's Guide	Sep 1998
Technical Report ITL-98-5	The Shear Ring Method and the Program Ring Wall	Sep 1998
Technical Report ITL-99-5	Rivet Replacement Analysis	Dec 1999
ERDC/ITL TR-00-1	Evaluation and Comparison of Stability Analysis and Uplift Criteria for Concrete Gravity Dams by Three Federal Agencies	Jan 2000